CALIFORNIA STATE UNIVERSITY, NORTHRIDGE

The Effects of Ocean Acidification and Eutrophication on the Macroalgae *Ulva* spp.

A thesis submitted in partial fulfillment of the requirements
For the degree of Master of Science in Biology

By

Leah Reidenbach

May 2017

The thesis of Leah Reidenbach is approved:

_____ _____

Dr. Robert Carpenter Date

_____ _____

Dr. Steve Dudgeon Date

_____ _____

Dr. Janet Kübler, Chair Date

California State University, Northridge

Acknowledgements

Thank you to my committee, Dr. Janet Kübler, Dr. Steve Dudgeon, and Dr. Robert Carpenter. Your guidance and commitment have been an invaluable asset to my success. Dr. Janet Kübler, thank you for your continuous support and encouragement. I appreciate our long discussions on macroalgal physiology which have helped me learn about the intricate and fascinating world of seaweeds. Dr. Steve Dudgeon, your enthusiasm and knowledge in statistics have increased my appreciation for experimental design and analysis. Thank you so much for your feedback throughout the process of analyzing the data from my experiments. Dr. Robert Carpenter, I will never forget the wonderful trips to San Simeon and Catalina Island where I learned so much about the ecology and identification of southern California seaweeds.

I want to acknowledge my lab mates Sam Scoma, Lissandra Gonzalez, and Courtney Button. My projects would not have been possible without your tremendous help and support. I am also grateful to the team of scientists who I worked with in Tasmania. Dr. Catriona Hurd, thank you for taking a chance with me and so kindly welcoming me into your lab. Working with you was an exceptional experience and wonderful opportunity. Dr. Pamela Fernández and Dr. Pablo Leal, thank you for all of your help in completing the *U. australis* project during my stay, but most importantly thank you for your friendship.

To my family and friends who supported me throughout this part of my journey in life, I am eternally grateful. Thank you for encouraging me to believe in myself. I can't imagine that I could have done this without your support. So I attribute, in part, the completion of this thesis to your kindness and love.

Table of Contents

List of Tables

List of Figures

Abstract

The Effects of Ocean Acidification and Eutrophication on the Macroalgae *Ulva* spp.

By

Leah Reidenbach
Master of Science in Biology

Ocean acidification is the increased absorption of atmospheric CO_2 in seawater and the consequent decrease in pH. This phenomenon is occurring throughout the global oceans while land use changes and large human populations near coasts are linked to increased nutrient concentrations in seawater. *Ulva* spp. blooms caused by nutrient enrichment occur regularly in some parts of the world and are known as green tides. There is concern that ocean acidification may increase green tides and intensify ecological and economic damages. *Ulva* spp. can utilize bicarbonate (HCO_3^-) as an inorganic carbon source, but this comes at an energetic cost as HCO_3^- must be converted to CO_2 before it can be used for carbon fixation. Therefore, increased utilization of pCO_2 with ocean acidification may benefit *Ulva* spp. Ocean acidification and eutrophication will occur simultaneously in many coastal ecosystems. The goal of the following investigations was to determine the effects of ocean acidification and nutrient enrichment alone and their interaction on photosynthetic, nutrient, and growth physiology of *Ulva* spp.

In Chapter 2, the response of *Ulva australis* to pH_T and ammonium (NH_4^+) enrichment were investigated in a seven day growth experiment using a range of pH_T (7.56 – 7.84) and ambient and enriched NH_4^+ concentrations. I measured relative growth rates (RGRs), NH_4^+ uptake rates and pools, photosynthetic characteristics, and tissue

carbon and nitrogen content. There was no interaction of pH_T and NH_4^+ enrichment on the physiological parameters. The RGR was not affected by pH_T, but was an average of two times higher in the enriched NH_4^+ treatment. $rETR_{max}$, total chlorophyll, and tissue nitrogen increased with both NH_4^+ enrichment and decreased pH_T. The C:N ratio decreased with decreasing pH and with NH_4^+ enrichment. Although $rETR_{max}$ increased and the C:N ratio decreased under decreased pH, these metabolic changes did not translate to higher growth rates. The results show that *U. australis* growth and physiology is more sensitive to NH_4^+ than it is to pH and that there is no interactive effect of NH_4^+ enrichment and decreasing pH.

In Chapter 3, *Ulva lactuca* was grown for 22 days under a range of pCO_2 and NH_4^+ concentrations and a multiple linear regression was used to analyze RGRs, NH_4^+ and NO_3^- pools, *in situ* NH_4^+ and NO_3^- uptake rates, tissue carbon and nitrogen content, carbohydrate and protein concentrations, and photosynthesis irradiance curves (P-I curves). The results from model selection and model-averaging techniques allowed me to make predictive models across a range of relevant ocean acidification and eutrophication scenarios and measure the effect sizes of pCO_2, NH_4^+ enrichment, and their interaction. Overall, there was no effect of pCO_2 and NH_4^+ on RGRs after day 5. However, there was a synergistic effect of pCO_2 and NH_4^+ enrichment on the growth rates during days 0 – 5. When pCO_2 and NH_4^+ concentrations increased simultaneously, NO_3^- uptake rates increased, which may have contributed to increased growth as seen in days 0 – 5. Maximum photosynthetic rates (P_{max}) decreased with increasing pCO_2 and there was a positive interaction of pCO_2 and NH_4^+ on Δ indicating CCMs were altered under these conditions. This shows that under high light intensities, P_{max} was negatively affected by

pCO_2 and CCMs are not altered when nutrients are limited. Ultimately, there was no longer-term effect of ocean acidification and eutrophication on *Ulva lactuca* growth.

Nutrient enrichment is a major cause of green tide blooms around the world and *Ulva australis* had the ability to enhance nutrient, photosynthetic, and growth physiology with NH_4^+ enrichment. Conversely, *Ulva lactuca* collected from a eutrophic environment, did not respond to NH_4^+ in terms of growth. Both chapters provided evidence that ocean acidification is unlikely to affect the growth rates of *Ulva* spp. However, the exception was a positive interactive effect of pCO_2 and NH_4^+ enrichment on the growth rate of *U. lactuca* during the first five days, suggesting ocean acidification could play a role in initiating *Ulva* spp. blooms in a eutrophic environment. This could be an important consideration for determining how green tides will be affected by ocean acidification in coastal areas where nutrient enrichment occurs in pulses, resulting in transiently increased nitrogen concentrations.

CHAPTER 1

Introduction

Coastal marine zones face many changes due to anthropogenic activities. Understanding how these changes affect species living in these zones creates an essential foundation for predicting how coastal ecosystems will change in the future. Atmospheric CO_2 is currently at the highest levels in recorded history and human population is rising. Consequently, CO_2 increases in the ocean, altering the carbonate system by increasing dissolved inorganic carbon (DIC) and CO_2, and reducing pH and carbonate (CO_3^{2-}). This process, termed ocean acidification, has biological effects on many marine biota (Fabry et al. 2008, Doney et al. 2009, Kroeker et al. 2013, Koch et al. 2013) which could be altered when coupled to other anthropogenic changes. As human population is expanding in coastal regions around the world, increases in processes such as land clearing, forestry, agriculture, grazing, industrialization, and the burning of fossil fuels (Vitousek et al. 1997) are linked to causing coastal eutrophication through inputs of new nitrogen (Paerl and Piehler 2008). Eutrophication affects the base of marine ecosystems by promoting the growth and reproduction of primary producers.

By the end of the 21st century, atmospheric CO_2 concentrations are expected to increase to over to >1000 ppm under baseline emission scenarios (business as usual or no mitigation) according to the Intergovernmental Panel on Climate Change (IPCC 2013). With it, the partial pressure of CO_2 (pCO_2) in surface seawater, which is in equilibrium with the atmosphere, will also increase (Doney et al. 2009). Studies on the effects of ocean acidification on non-calcareous, fleshy macroalgae have shown they may benefit

through enhanced carbon fixation and growth rates (Cornwall et al. 2012, Kroeker et al. 2013, Johnson et al. 2014).

The responses of organisms to environmental changes are most often assessed by evaluating one abiotic change in a controlled laboratory setting (Todgham and Stillman 2013). While this can be informative for determining effects on physiological processes, it does not elucidate how organisms will respond in the natural environment where multiple abiotic changes may occur simultaneously. Thus, it is necessary to study the effects of multiple predicted stressors and drivers if the goal is to understand responses of populations in their natural habitats.

Study species

Ulva spp. (Chlorophyta) (Fig 1.1) are the predominant species in large accumulations of unattached green macroalgae around the world known as green tides (Ye et al. 2011). The most prolific examples of green tide blooms include the annual occurrence in Brittany, France where massive amounts (up to 74,000 m^3) of drifting algae wash up sandy beaches and bays (Perrot et al. 2014). In Qingdao, China 1,200 km^2 of *Ulva prolifera* accumulated in the Yellow Sea preceding the 2008 Olympic sailing competition causing massive cleanup efforts and economic consequences (Liu et al. 2009, Gao et al. 2010). Green tides have ecological consequences due to their large influence on seawater chemistry, causing fluctuating pH, hypoxia, the release of secondary compounds, and nutrient depletion (Van Alstyne et al. 2015). They also smother seagrass beds, cause foul odors, reduce benthic diversity, and impact fisheries and tourism (Teichberg et al. 2010, Smetacek and Zingone 2013).

Ulva spp. were chosen as a model organism for studying the interacting effects of ocean acidification and eutrophication because of its role as common bloom forming species. *Ulva* spp. morphology contribute to their ability to obtain light and nutrients (Littler and Littler 1980). They have a distromatic thallus (two cell layers) and a large surface area to volume ratio which is favorable for increased nutrient uptake rates (Pedersen and Borum 1997). Under eutrophic conditions *Ulva* spp. exhibit high growth rates and therefore are good at reflecting environmental changes. Their ubiquity in the environment and their tissue N and chlorophyll levels make them useful for determining nitrogen availability in seawater, making them a good indicator species (Barr 2007). *Ulva* spp. can be found worldwide, and there are 594 species listed on AlgaeBase, of which 129 are taxonomically accepted (Guiry and Guiry 2016).

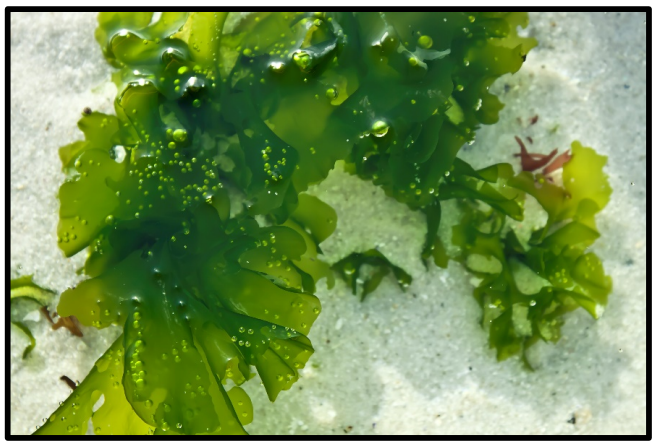

Fig 1.1: Typical morphotype of *Ulva* spp. found in temperate and tropical coastal zones around the world. Bay of Fires Conservation Area, Tasmania, Australia.

The well-developed carbon concentrating mechanisms (CCMs) in *Ulva* spp. make them an important species for studying ocean acidification effects on macroalgae. Despite the low concentration of dissolved CO_2 in seawater, many macroalgae are still able to saturate photosynthetic enzymes with CO_2 because of their ability to use HCO_3^-, another form of DIC. It has been demonstrated that *Ulva* spp. can switch from using CCMs to

diffusive uptake of CO_2 when the pH of the seawater decreases and pCO_2 increases (Axelsson et 1999, Björk et al 1993) or utilize both HCO_2 and CO_2 through intermediate use of CCMs and diffusive uptake (Cornwall et al. 2012, Young and Gobler 2016). The energetic savings from decreasing CCMs under increased pCO_2 may be able to go towards other metabolic activities such as growth (Giordano et al. 2005).

Objectives

This research topic explores the effects of two combined environmental changes, ocean acidification and eutrophication on a common green macroalgal species. The experiments were designed to determine the effects of CO_2 enrichment and NH_4^+ enrichment alone as well as their interactive effect on the growth, nutrient, and photosynthetic physiology of the algae. I have taken two approaches to researching this topic. First, a short-term study was completed in an ocean acidification culture system in Hobart, Tasmania on *Ulva australis.* In this study, the effect of pH was measured in ambient and enriched NH_4^+ treatments. Photosynthesis and nutrient utilization were evaluated along with growth rates to determine the effects of ocean acidification and NH_4^+ enrichment on the physiology of *U. australis*. The second approach used a flow-through culture system to evaluate longer-term (three weeks) physiological responses to ocean acidification and NH_4^+ enrichment across a range of pCO_2 and NH_4^+ concentrations in two trials. The data from the experiment were used to estimate effect sizes of ocean acidification, eutrophication, and their interaction on algal physiology and growth and to make predictive models based on their responses. Both approaches contribute to increasing our understanding of how opportunistic macroalgae species may respond under future oceanic conditions.

Chapter 2
The Effects of pH and Ammonium Enrichment on the Macroalga *Ulva australis* (Chlorophyta).

Introduction

The burning of fossil fuels has caused an increase in atmospheric CO_2 concentration that has not been experienced in at least the past 800,000 years (Lüthi et al. 2008). Since the industrial revolution (ca. 1760), the atmospheric CO_2 concentration has increased from 280 μatm to over 400 μatm, and about 30% of additional atmospheric CO_2 has been absorbed into the ocean (IPCC 2015). Increasing pCO_2 in seawater reduces pH and the carbonate ion (CO_3^{2-}) concentration and increases bicarbonate (HCO_3^-) and dissolved CO_2 concentrations. These changes in the concentrations of dissolved inorganic carbon (DIC) may differentially affect marine phototrophs which utilize DIC through various mechanisms of carbon acquisition (Giordano et al. 2005, Hurd et al. 2009).

The enzyme responsible for carbon fixation, ribulose bisphosphate carboxylase-oxygenase (RUBISCO), first appeared in photosynthetic organisms in a high-CO_2 /low-O_2 environment about 2.4 billion years ago (Raven et al. 2012). Its dual roles as a carboxylase and oxygenase result in competitive inhibition of carboxylation by oxygenation (Bowes 1991). In most algae, carbon concentrating mechanisms (CCMs) increase CO_2 in the chloroplast to concentrations higher than is possible via diffusion of dissolved CO_2 alone, impeding photorespiration (Giordano et al. 2005). CCMs are very common in seaweeds. Using the pH-drift method, 82 – 90% of macroalgal species from the phyla Rhodophyta, Ochrophyta, and Chlorophyta have been found to exhibit CCMs (Maberly 1990, Stepien 2015). However, low-light habitats have been shown to favor high abundances of non-CCM using algae (Cornwall et al. 2015). Macroalgae with

CCMs have been shown to have photosynthetic rates saturated with inorganic carbon supply at the current pCO_2 (Beer and Koch 1996, Beardall et al. 1998, Israel and Hophy 2002).

Although photosynthetic rates are typically carbon saturated at air equilibrium, the growth rate of macroalgal species is sometimes affected by increasing pCO_2. *Hizikia fusiforme* growth rates increased under elevated pCO_2 while maximum photosynthetic rates were the same under ambient air and pCO_2 enriched treatments (Zou 2005). Growth rates of *Gracilaria chilensis* and another *Gracilaria* sp. were enhanced by elevated pCO_2 (Gao et al. 1993). *Gracilaria lemaneiformis* growth rates were also enhanced under increased pCO_2, but only at an intermediate photon flux density (PFD) (160 μM photons m^{-2} s^{-1}) (Zou and Gao 2009). *Ulva* spp. growth rates have been shown to increase or be unaffected by increased pCO_2 (Gordillo et al. 2001, Olischläger et al. 2013, Andría et al. 2001, Rautenberger et al. 2015, Liu and Zou 2015). The growth rates of thirteen species of algae, including green, red, and brown algae, had no response to elevated pCO_2 with the exception of *Hypnea musciformis,* which exhibited negative growth rates under elevated pCO_2 (Israel and Hophy 2002). Differences in responses to pCO_2 manipulation seen in seaweed species having CCMs may be caused in part by unsuitable nutrient concentrations, temperature, and/or PFD for the seaweeds to support higher growth rates.

Primary production and cellular respiration can lead to a diurnal or seasonal pH change in kelp forests, seagrass beds, and macroalgal beds (Duarte et al. 2013, Delille and Borges 2009, Frankignoulle and Bouquegneau 1990, Middelboe and Hansen 2007, Wootton et al. 2008). Few experiments have manipulated pH and pCO_2 to include the diurnal fluctuations that occur in those high productivity, high photosynthetic biomass

environments (McElhany and Busch 2013). Culture experiments with macroalgae typically exhibit diurnal fluctuations in pH due to CO_2 uptake and release by the organism in an enclosed volume of water. I was able to accurately monitor this fluctuation throughout the duration of the experiment on small timescales. Laboratory experiments that mimic natural variation in pH may be able to better represent how organisms will respond to decreases in pH in the natural environment (Cornwall et al. 2012).

In addition to excess CO_2 gas entering from the atmosphere, coastal regions receive inputs of excess nitrogen from aquaculture, agricultural, wastewater treatment, and the burning of fossil fuels (Paerl 1997, Anderson 2002). Excess nitrogen can increase primary production and, in some cases, stimulate algal blooms (Valiela et al. 1997, Li et al. 2016, Smetacek and Zingone 2013). The response of algae to increased pCO_2 (resulting in decreased pH) is potentially regulated by nitrogen availability, as protein synthesis requires both nitrogen and carbon skeletons (Gordillo et al. 2001, Turpin 1991). In the case of macroalgae with CCMs, a reduction in CCM activity under elevated pCO_2 could result in energetic savings, which may be utilized for protein synthesis and growth when nutrients are not limiting. *Ulva lactuca*, *Gracilaria* spp., and *Hizikia fusiforme* grown with elevated pCO_2, had enhanced nitrate (NO_3^-) uptake rates (Zou 2005, Gao et al. 1993, Gordillo et al. 2001). However, NO_3^- uptake rates decreased with elevated pCO_2 in *G. tenuistipitata* and *G. gaditata* (Garcia-Sanchez et al. 1994, Andría et al. 1999).

NH_4^+ is typically the preferred form of nitrogen because it is requires less energy than NO_3^- assimilation, as NO_3^- must first be reduced via nitrate reductase activity (NRA) for assimilation (Syrett 1981). Although NO_3^- is the most abundant and common form of

dissolved inorganic nitrogen (DIN) in the ocean, increasing human population densities on coasts, land use change, and decreasing ocean pH all increase the availability of NH_4^+ in coastal areas (Paerl and Piehler 2008). The interacting effects of NH_4^+ and pH on the growth and photosynthesis of macroalgae have been less thoroughly investigated than have the interacting effects of NO_3^- and pH (Gordillo et al. 2001, Young and Gobler 2016).

Ulva spp. are opportunistic under eutrophic conditions (Teichberg et al. 2010) and have potentially increased growth rates under elevated pCO_2 alone (Gordillo et al. 2001, Olischläger et al. 2013). To determine if there is an interactive effect between these two environmental trends (decreasing pH and elevated NH_4^+ concentration) on growth, nutrient, and photosynthetic physiology of *Ulva australis*, I grew them in seawater with ambient and enriched NH_4^+ concentrations across a range of pH_Ts. The pH_T of seawater in the algal growth chambers was allowed to fluctuate in response to algal metabolism, producing diurnal pH_T variations as seen in natural populations (Wootton et al. 2008). Using a newly designed culture system, I was able to measure the pH_T within each of 24 culture chambers at a frequency of at least 3 hours throughout the week-long experiment, monitoring the effect of *U. australis* photosynthesis and respiration on seawater pH_T.

I hypothesized that: there would be no effect of pH on the photosynthetic characteristics ($rETR_{max}$, α, β, and E_k) of *Ulva australis*, because it has an efficient CCM and is not limited for DIC at present pCO_2. I expected the growth rate to increase with decreasing pH based on previous research (Gordillo et al. 2001, Olischläger et al. 2013, Young and Gobler 2016). NH_4^+ enrichment alone was expected to increase the growth rate, photosynthetic light harvesting efficiency, chlorophyll content and increase the

internal NH_4^+ pools of *U. australis* as has been shown for other *Ulva* species (Teichberg et al. 2010, Dailer et al. 2012). I hypothesized a positive interactive effect of pH and NH_4^+ enrichment on *U. australis* that would increase growth rates more than either factor alone. I predicted a negative relationship between pH and NH_4^+ uptake rates such that NH_4^+ uptake rates increase with decreasing pH. Increased availability of dissolved CO_2 in the DIC and increased NH_4^+ uptake rates could be evident in C and N content of the algae and the internal NH_4^+ pools. *Ulva* spp. with high C and N content, having adequate internal supply of nitrogenous and carbon skeleton precursors, are poised to rapidly exploit changes in light and temperature, potentially leading to green tide bloom conditions.

Methods

Collection and acclimation

Ulva australis was collected from Blackmans Bay, Tasmania, Australia (42°59'56"S 147°19'8"E) in July 2015 (winter). Algae were stored on ice in plastic zip-lock bags and returned to the laboratory within five hours of collection. All visible epiphytes were carefully removed from the surface of the blades which were then rinsed with filtered seawater. They were kept under 200 μmol photons m^{-2} s^{-1} at 16.6°C with a 12h:12h light dark cycle in aerated seawater for 3 days to acclimate them to laboratory conditions.

Experimental design

Three *Ulva australis* thalli with a total fresh weight of 1.07 ± 0.02 g were placed in each 650 mL chamber filled with 600 mL of seawater that was UV-sterilized and filtered through a 1 μm-filter (Polyester Felt Filter Bags**,** NETCO, Hobart, Australia). The

seaweeds were grown in the chambers for seven days in a 16.6°C temperature controlled room under 200 μmol photons m^{-2} s^{-1} (measured using a 4π Li-Cor LI-193 Spherical Quantum Sensor connected to a LI‑250A portable light meter) and a 12h:12h light dark cycle. Experimental chambers were randomly assigned to one of the treatments, which consisted of a range of pH_T crossed with ambient and enriched NH_4^+ concentrations for a total of 24 chambers. The average pH_T of each chamber was determined from measurements of pH_T during the dark cycle throughout the entire experiment.

pH_T was measured in each of the 24 growth chambers every 1.5 – 3 hours using a modified version of the automated spectrophotometric pH_T measurement system (McGraw et al. 2010). Briefly, a syringe pump (V6 pump with valve 24090, Norgren, UK) and two 12-port rotary valves (23425 valve driver with valve 24493, Norgren, UK) were used to sample seawater directly from each growth chamber. For each spectrophotometric pH measurement, a reference spectrum was acquired after flushing 25 mL of seawater through a 1 cm flow-through quartz cuvette. A spectrum (400 – 800 nm) was acquired using an LED light source and a UV-Vis spectrometer (BluLoop and USB2000+, Ocean Optics, USA). A dye + seawater spectrum was then obtained after mixing 200 μL of 2 mM metacresol purple sodium salt dye (211761-10G, Sigma Aldrich, Australia) with an additional 25 mL of seawater within the syringe pump. The two spectra were used to calculate an absorbance spectrum. pH_T was calculated using the quadratic fits of the absorbance spectra between 429 – 439 nm, 573 – 583 nm and a background signal averaged between 750 – 760 nm. When compared to calculations based on a single wavelength, the quadratic fit approach leads to a three-fold improvement in measurement precision (McGraw et al. 2010). Each recorded pH_T was

the average of four replicate measurements, which took approximately 3 minutes to obtain. The temperature of each sample was recorded with a PT100 temperature sensor and a high-precision data logger (PT-104, PICO Technology, UK). All instrument control, spectra manipulations, and pH_T calculations were done using LabVIEW 2014 (National Instruments, USA).

Peristaltic pumps (FPU500, Omega Engineering, USA) were used to provide fresh seawater to each growth chamber at a rate of 6 – 8 mL/min. The pH_T of seawater pumped to each tank was maintained using a control system similar to that described in (Bockmon et al. 2013). Seawater entering each growth chamber was equilibrated with a N_2/CO_2 gas mix using a membrane contactor (Micromodule, model 0.5X1, Membrana, USA). The appropriate mix of N_2 and CO_2 gas achieved for each of the pH_T treatments using three pairs of mass flow controllers (FMA5418A and FMA545C, Omega Engineering, USA). The flow rate of each mass flow controller is proportional to the input voltage, which was supplied by an analog output module housed in a USB chassis (NI9264 and cDAQ-9174, National Instruments, USA).

The ambient concentration of NH_4^+ was < 0.5 μM and the elevated concentration of NH_4^+ was achieved using an auto-dosing peristaltic pump (Jebao DP-4) programmed to deliver 12 mL of a 1000 μM NH_4Cl solution to growth chambers every two hours. Based on NH_4^+ dosing rate, the NH_4^+ concentration in the elevated treatment was 20 μM.

Growth rates

Ulva australis thalli were blotted with tissue to remove excess water and weighed before the start of the experiment and after seven days. The total weight of the three thalli from each chamber was used for the analysis. The relative growth rate (RGR), expressed

as % day^{-1}, was calculated as RGR = $\ln(FW_f/FW_i) \times t^{-1} \times 100$ where FW_i is the initial fresh weight, and FW_f is the final fresh weight after t days. Each of the three *U. australis* pieces were randomly selected for various measurements. The first piece was used to determine nutrient uptake rates, the second piece was used to determine chlorophyll fluorescence and was then sampled for photosynthetic pigments, and the third piece was divided into subsamples for NH_4^+ pools, and tissue C and N composition.

NH_4^+ uptake rates

At the end of the seven-day incubation period, one of the three *Ulva australis* thalli (0.43 ± 0.03 g of FW) was removed from each chamber to an Erlenmeyer flask containing 200 mL of filtered seawater. The seawater in each flask was obtained from the automated pH control system so that the pH_T of the seawater in the nutrient uptake experiment matched the pH_T of the experimental treatment. The initial NH_4^+ concentration was 20 µM with overhead light of 200 µmol photons m^{-2} s^{-1}. Flasks were placed on an orbital shaker (RATEK OM7, Victoria, Australia) set to 80 rpm and continuously stirred to induce water motion and reduce boundary layer effects (Hurd 2000). A 10 mL sample of the water was taken at 0 and 30 minutes, and frozen at -20°C, until defrosted and analyzed for NH_4^+ concentration using a QuickChem 8500 series 2 Automated Ion Analyzer (Lachat Instrument, Loveland, USA). The uptake rate (V) was determined according to Pedersen (1994) using the formula $V = [(S_i \times vol_i)-(S_f \times vol_f)]/(t \times FW)$ where S_i and S_f are the initial and final NH_4^+ concentrations (µM) over a period of time (t), vol is the seawater volume in the flask and FW is the fresh weight (g) of the algae.

Internal soluble NH_4^+ pools

The boiling water extraction method was used to determine the internal soluble NH_4^+ pool (Hurd et al.1996). A 0.18 ± 0.01 g FW piece of *Ulva australis* was put in a boiling tube with 20 mL of deionized water then placed in a boiling water bath for 40 minutes. The liquid was cooled, decanted, and then filtered through a 0.45 μm Whatman filter (GF/C). This process was repeated on the same algal piece three times and the concentration of internal soluble NH_4^+ pools was calculated using the sum of the NH_4^+ concentrations of the three water samples of each algal piece. NH_4^+ concentrations were measured as stated above.

Photosynthetic pigments

Following the experiment, a 0.04 ± 0.001 g FW piece of *Ulva australis* from each experimental chamber was kept at -20°C pending analysis. Each sample was then ground in 5 mL of 100 % ethanol with a ceramic mortar and pestle in dim light and with the samples shaded. The extract was poured into 10 mL centrifuge tubes and placed in the dark at 4°C for six hours. Samples were then centrifuged for 10 min at 4000 rpm at 4°C. Total Chl *a* and *b* concentrations in the supernatant were determined according to the quadrichroic formula from Ritchie (2008) using a spectrophotometer (S-22 UV/Vis, Boeco, Germany).

Rapid light curves

Chlorophyll fluorescence of photosystem II was measured using a Pulse Amplitude Modulation fluorometer (diving-PAM, Walz, Germany) to generate rapid light curves and obtain measurements of the maximum quantum yield of PSII photochemistry (F_v/F_m), which is used as an indicator of stress (Baker 2008). On day

seven of the experiment, one thallus from each chamber was dark adapted for 20 minutes before exposure to a flash of saturating light to obtain maximum fluorescence (F_m). Then a rapid light curve was generated by increasing exposure to photosynthetic active radiation (PAR) ranging from 0 - 422 μM photons m^{-2} s^{-1}. F_v/F_m was calculated by the equation F_m-F_0/F_m, were F_0 is the fluorescence under measuring light conditions (ca. 0.15 μmol photons m^{-2} s^{-1}) and F_m is the maximum fluorescence under saturating light conditions. Relative ETR (rETR) was calculated by the equation rETR = Y * PAR * 0.5. A hyperbolic curve was fit to the rETRs generated by each rapid light curve using a modified equation of Walsby (1997), $rETR_c = rETR_{max} (1 – \exp (-\alpha I / P_m)) + \beta I$, where $rETR_c$ is the calculated rETR, $rETR_{max}$ is the maximum ETR at light saturating PFDs, α is the initial slope of the curve during light-limiting PFDs, and β is the slope of photoinhibition at high PFDs. The coefficients used in the equation were calculated using a least squares method (Walsby 1997).

Total carbon and nitrogen content

A 0.35 ± 0.03 g FW section was dried at 60°C overnight, ground to a fine powder, and then analyzed for total tissue carbon and nitrogen content. Samples were weighed into pressed tin capsules (5x8 mm, 0.2 mg; Sercon, U.K.). Carbon and nitrogen content were determined using a Fisons NA1500 elemental analyzer coupled to a Thermo Scientific Delta V Plus via a Conflo IV. Combustion and reduction were achieved at 1020 °C and 650 °C respectively. Percent C and N composition was calculated by comparison of mass spectrometer peak areas to those of standards with known concentrations.

Data analysis

An analysis of covariance (ANCOVA) was used to test for the interacting effect of pH and NH_4^+ on physiological responses of *U. australis*. pH_T was used as the continuous factor (i.e., the covariate) and NH_4^+ was used as the categorical variable. First, the interacting term was tested for a significant interaction. If there was not a significant interaction, it was dropped from the model to determine the effects of each factor alone. Outliers greater than 3 standard deviations from the mean were removed *a priori* and are indicated in the figures (Fig 3B). ANCOVA assumptions were checked using a Shapiro-Wilk test of normality and Cochran's Q test for homogeneity of variances. Statistical analyses were done using the statistical software R studio.

Results

pH_T

The pH_T given for each treatment is the average value from the nighttime (dark) pH_T measurements in each culture chamber. The measurements oscillated around the gas mixers' set points due to algal metabolism: during the light period pCO_2 decreased, increasing pH_T; during the dark period cellular respiration produced CO_2, deceasing pH_T, with pH_T being stable throughout the nighttime (Fig 2.1).

Interactive effects

The slopes for all dependent variables were indistinguishable between ambient and enriched NH_4^+ treatments as indicated by the non-significant interaction terms (pH_T x NH_4^+) in the ANCOVAs (Table 2.1). The following results for all dependent variables are ANCOVAs with the interaction term dropped from the model.

Relative growth rate

Relative growth rates of *Ulva australis* in high NH_4^+ treatments (8.75 ± 0.69 % day^{-1}) were double those in low NH_4^+ treatments (4.36 ± 0.5 % day^{-1}) (ANCOVA; $F_{1, 21}$ = 25.43, p<0.001, Fig 2.2). Growth rates did not differ across pH_T treatments (ANCOVA; $F_{1, 21}$ = 2.65, p=0.118).

NH_4^+ uptake rates

NH_4^+ uptake rates were lower in *U. australis* from the enriched NH_4^+ treatment (9.06±1.04 µmol NH_4^+ g^{-1} FW $hour^{-1}$) than in the ambient NH_4^+ treatment (13.42±0.97 µmol NH_4^+ g^{-1} FW $hour^{-1}$)(ANCOVA; $F_{1, 21}$ = 7.74, p=0.013, Fig 2.3A). pH_T had no significant effect on the NH_4^+ uptake rates (ANCOVA; $F_{1, 21}$ = 2.90, p=0.104).

Internal NH_4^+ pools

As expected, internal NH_4^+ pools in *U. australis* thalli were higher in the enriched NH_4^+ treatments (75.21±8.85 µmol NH_4^+ g^{-1} FW) than in the ambient NH_4^+ treatment (39.60±4.81 µmol NH_4^+ g^{-1} FW) (ANCOVA; $F_{1, 20}$ = 14.34, p=0.001, Fig 2.3B). pH_T had no effect on the NH_4^+ pools (ANCOVA; $F_{1, 20}$ = 0.02, p=0.894).

Photosynthetic pigments

The total chlorophyll concentration (Chl *a* + *b*) content was higher in *U. australis* from enriched NH_4^+ treatments (1.27±0.07 mg g^{-1} FW) compared to the ambient NH_4^+ treatment (0.86±0.08 mg g^{-1} FW) (ANCOVA; $F_{1, 21}$ = 10.93, p=0.003, Fig 2.4A). The total chlorophyll concentration also increased with decreasing pH_T (ANCOVA; $F_{1, 21}$ =7.37, p=0.013) (regression; r^2=0.18 p=0.035).

Rapid light curves

$rETR_{max}$, $F_v/F_{m,}$ E_k, α, and β were assessed with rapid light curves. $rETR_{max}$ increased with with NH_4^+ enrichment (ANCOVA; $F_{1, 21}$ =33.20, p<0.001, Fig 2.4B) with an average $rETR_{max}$ of 4.96±0.58 in the ambient NH_4^+ treatment and 11.9±0.94 in the enriched NH_4^+ treatment. $rETR_{max}$ increased with decreasing pH (ANCOVA; $F_{1, 21}$ =2.67, p<0.001) (regression; r^2=0.9497 p<0.001). Like $rETR_{max}$, the average F_v/F_m was higher with NH_4^+ enrichment and decreasing pH (ANCOVA; $F_{1, 21}$ =25.71, p<0.001 and ANCOVA; $F_{1, 21}$ =13.29, p=0.001, respectively, Fig 2.4C) (regression for pH; r^2=0.2279 p=0.018). The F_v/F_m in the ambient NH_4^+ treatment was 0.59±0.22 and 0.74 ± 0.01 in the enriched NH_4^+ treatment.

NH_4^+ enrichment had no significant effect on E_k (ANCOVA; $F_{1, 21}$ =0.22, p=0.643)(Fig 2.5A), while pH_T did have a significant effect (ANCOVA; $F_{1, 21}$ =4.38 p=0.049). As pH_T decreased, E_k increased (regression; r^2=0.99, p<0.001). α was not influenced by pH_T (ANCOVA; $F_{1, 21}$ =0.08, p=0.785)(Fig 2.5B). However, α was greater with NH_4^+ enrichment (ANCOVA; $F_{1, 21}$ =7.25, p=0.014) with a mean of 0.14±0.03 in the ambient NH_4^+ treatment and a mean of 0.22±0.01 in the enriched ammonium treatment. Likewise, β was not influenced by pH_T (ANCOVA; $F_{1, 21}$ =0.84, p=0.37) (Fig 5C) but β was more negative in the enriched NH_4^+ treatments, averaging -0.008±1.58x10^{-3} in the ambient NH_4^+ treatment down to -0.0013±8.48x10^{-4} in the enriched NH_4^+ treatment (ANCOVA; $F_{1, 21}$ =10.11, p=0.005).

Tissue carbon and nitrogen

Tissue C (% DW) was not affected by pH or NH_4^+ enrichment (ANCOVA; $F_{1, 21}$ =1.08, p=0.310 and $F_{1, 21}$=0.38 p=0.542, respectively) (Fig 6A). Tissue N (%DW)

averaged 1.39±0.06 in the ambient NH_4^+ treatment and was significantly greater in the enriched NH_4^+ treatment with an average of 2.56±0.14 (ANCOVA; $F_{1, 21}$=56.24, p=<0.001)(Fig 6B) and increased as pH decreased (ANOVA; $F_{1, 21}$=12.52, p=0.0019). The C:N ratio was lower in enriched NH_4^+ treatment with an average of 11.3±1.15, while in the ambient NH_4^+ treatment the average was 21.87±0.95 (ANCOVA; $F_{1, 21}$ =63.47, p=<0.001)(Fig 6C). The C:N ratio decreased with decreasing pH (ANOVA; $F_{1, 21}$ =13.23, p=0.0015).

Discussion

There was no interactive effect of pH and NH_4^+ enrichment on *Ulva australis* for RGR or any of the variables measured, making it possible to analyze the effects of pH and NH_4^+ enrichment individually (Table 2.1). These results are in accordance with Young and Gobler (2016) who found no interactive effects of environmentally relevant levels of pCO_2 and NO_3^- enrichment on growth and tissue carbon and nitrogen composition across multiple seasons for *Ulva* spp. However, these findings contrast those of Gordillo et al. (2001), who found that at a highly elevated pCO_2 (10,000 ppm), *U. rigida* growth rates, nitrate reductase activity, biochemical composition, and photosynthetic responses depended on NO_3^- enrichment. Further, Gordillo et al. (2003) found that *U. rigida* chlorophyll fluorescence responses to elevated pCO_2 (10,000 ppm) were also dependent on NO_3^- enrichment. The predicted end of the century decrease of ~0.3 – 0.5 pH is due to increased levels of atmospheric pCO_2 to ~ 1000 ppm (Caldeira 2005). At ecologically relevant levels, the effects of ocean acidification on *Ulva* spp. growth and physiology will likely not be dependent nutrient enrichment due to NO_3^- or NH_4^+.

Growing with NH_4^+ enrichment affected all variables measured in *Ulva australis*, except E_k and tissue C content. NH_4^+ enrichment increased RGRs to twice that of *U. australis* grown in non-enriched seawater (Fig 2.2). Increased RGR with increasing nutrient concentrations is common for *Ulva* spp. Growth increased with increasing NO_3^- concentrations for *Ulva intestinalis* up to 600 μM NO_3^-, while growth at concentrations above 600 μM NO_3^- decreased relative to peak growth (Fong et al. 2004). When *Ulva lactuca* was exposed to wastewater effluent with 35 μM total nitrogen (TN), growth increased by approximately 235% relative to the control which had 5.6 μM TN (Dailer et al. 2012). Similarly, growth rates of *U. lactuca* more than doubled with the addition of NH_4^+ or NO_3^- when collected from an oligotrophic site, but an increased growth rate with nutrient enrichment was not evident when algae were collected from a nutrient enriched site (Teichberg et al. 2008). Furthermore, Lapointe and Tenore (1981) showed that when *Ulva fasciata* was not grown with sufficient light, the enhancement of growth with NO_3^- was eliminated. Thus, nitrogen enrichment is typically related to increased growth of *Ulva spp.*, but this is likely dependent on seasonal changes in light supply and ambient nitrogen levels (Fong et al.1998).

In the present experiment, internal NH_4^+ pools and tissue N content were nearly twice as large in the NH_4^+ enriched treatments as in the ambient treatments (Fig 2.3B and Fig 2.6B, respectively), indicating light and nutrients were sufficient for nutrient assimilation and growth, while the ambient NH_4^+ treatments were N-limiting. In the NH_4^+ enriched treatment, *Ulva australis* NH_4^+ uptake rates were slower than in the ambient NH_4^+ treatments (Fig 2.3A), which supports the theory that nutrient histories influence nutrient uptake capabilities by feedback inhibition as internal N pools increase (D'Elia

and DeBoer 1978, Fujita 1985, McGlathery et al. 1996, Fong et al. 2003, Teichberg et al. 2007, Kennison et al. 2011). *U. australis* from the NH_4^+ enriched treatments, were still capable of NH_4^+ uptake despite growth under high nutrient availability and relatively concentrated NH_4^+ pools. This has also been demonstrated with *Ulva expansa* and *Ulva intestinalis* with varying nutrient histories (Kennison et al. 2011) and shows their ability to take up surplus nutrients under growth with low and high nutrient concentrations.

NH_4^+ enrichment increased total chlorophyll concentrations, $rETR_{max}$, and the maximum quantum yield of PSII photochemistry (F_v/F_m). The efficiency of light harvesting (α) increased with NH_4^+ enrichment indicating N-deficiency inhibited photosynthesis (Fig 2.5B). N-deficiency has been shown to lower the ability of *Ulva rotundata* to photoacclimate to changing light regimes and can lead to declines in $rETR_{max}$ and α in *U. lactuca* (Dalier et al. 2012, Chen et al. 2015). Photoinhibition (β) and differences in β between NH_4^+ enriched and ambient treatments were small at the highest PFDs measured which suggests an increased range of PFD would be better suited for demonstrating differences in β that are biologically meaningful. Nutrient enrichment increased growth and photosynthetic characteristics of *U. australis* in this study which has been shown with many macroalgae (Valiela et al. 1997).

The increased chlorophyll content with decreasing pH (Fig 2.4A) agrees with Chen et al. 2015 who found that Chl *a* increased with CO_2 enrichment and $rETR_{max}$ was correlated with Chl *a.* In this experiment, the increased total chlorophyll concentrations support the increased $rETR_{max}$, E_k, and F_v/F_m found with *U. australis* in decreased pH. These results contrast other experiments which found that chlorophyll concentrations

decreased with decreased pH (Olischläger et al. 2013, Gordillo et al. 2003, Stengel et al. 2014) or were not affected (Rautenberger et al. 2015, Liu and Zou 2015)

I hypothesized that the RGR would increase with decreasing pH, but found no effect of pH on growth rates. A decoupling of the photosynthetic characteristics and growth rates is not uncommon because growth is linked to multiple components of algal metabolism, not just a single process (i.e., photosynthesis). In this experiment, this decoupling may represent a tradeoff between nitrogen resources for improved photosynthetic efficiency (higher concentration of chlorophyll) or growth (resulting in dilution of chlorophyll with cellular division). Zou 2005 found that the growth rate of *Hizikia fusiforme* increased while maximum photosynthetic rates were unaffected by increased pCO_2. Liu and Zou (2015) demonstrated that the photosynthetic rates of *Ulva lactuca* had increased and growth rates were unaffected by CO_2 enrichment at 25°C. However, both photosynthetic rates and growth rates were unaffected with CO_2 enrichment at 15°C, indicating that temperature plays an important role in determining photosynthetic rate regulation by DIC concentration. *Ulva rigida* growth rates were shown to be unaffected by pCO_2, but did increase with increased PFD (Rautenberger et al. 2015).

The supposition that macroalgal growth rates may increase with future changes in ocean chemistry (i.e., decreased pH, increased pCO_2) due to energy savings from downregulation of CCMs (Raven et al. 2011, Hepburn et al. 2011, Koch et al. 2013) is likely not a pervasive feature of CCM utilizing macroalgae. Enhanced growth with pCO_2 enrichment is probably the result of the influence of light levels on CCMs (Kübler and Raven 1995, Pedersen and Borum 1997). Energetic constraints on carbon acquisition at

low PFDs increases dependence on passive CO_2 diffusion, while CCMS are more efficient at high PFD (Hepburn et al. 2011). When PFD is low, the carbon demands of photosynthesis can be saturated by diffusion alone and CCMs are not needed. For example, pCO_2 enrichment only enhanced *Gracilaria lemaneiformis* growth rates at an intermediate PFD (Zou and Gao 2009). There was no evidence of decreased pH benefiting *Ulva australis* RGR in this experiment, but the C:N ratio decreased indicating that lower pH may provide relief from nutrient limitation.

Nitrogen content of the dried tissue increased with decreasing pH (Fig 2.6B). This was in contrast to studies examining the effects of NO_3^- enrichment in *Ulva* spp. where decreasing pH did not increase nitrogen content (Gordillo et al. 2001, Young and Gobler 2016). Compared to NO_3^-, NH_4^+ enrichment may cause different effects on tissue N with decreasing pH because *Ulva* spp. have a higher affinity for NH_4^+ than for NO_3^- (Pedersen and Borum 1997, Fan et al. 2014).

Although N content increased, internal NH_4^+ pools were not affected by decreasing pH. An increase in chlorophyll content and tissue N with decreasing pH supports the hypothesis that NH_4^+ was assimilated to produce nitrogenous compounds such as chlorophyll, protein, and amino acids and not stored in internal NH_4^+ pools. I did not detect changes in NH_4^+ uptake rates with decreasing pH, which corresponds to the absence of changes in NH_4^+ pools and growth rates. This contrasts findings of increased NO_3^- uptake rates with increasing pCO_2 in *Ulva rigida*, *Hizikia fusifome*, and *Gracilaria* spp. (Zou 2005, Gao et al. 1993, Gordillo et al. 2001), and NH_4^+ uptake rate increased with elevated pCO_2 in *Hypnea spinella* (Suárez-Álvarez 2012). The effect of pH/pCO_2 on

N uptake rate may also be sensitive to temperature, as NO_3^- uptake rates in *Ulva lactuca* increased with CO_2 enrichment at 25°C, but not 15°C (Liu and Zou 2015).

This study adds to our understanding of how *Ulva* spp. will respond to reduced pH and increased NH_4^+ concentrations. The response of *Ulva australis* to reduced pH in this study corroborates with other results that increasing CO_2 will likely not have an impact on *Ulva* growth rates (Israel and Hophy 2002, Andría et al. 2001, Rautenberger et al. 2015, Liu and Zou 2015), although *Ulva* spp. growth rates have also been reported to respond positively to decreasing pH (Olischläger et al 2013, Xu and Gao 2012). Given that all *Ulva* spp. have relatively simple morphologies and similar carbon and nitrogen metabolisms it is likely that environmental variables, such as light and temperature, are essential to mediating responses to decreased pH with phenomenon such as OA.

Young and Gobler (2016) found that *Ulva* spp. growth rates increased with pCO_2 enrichment but varied by season, primarily increasing only in summer months. *U. australis* from this experiment were collected during winter months and had no growth response to decreased pH. Assuming their findings are representative of *Ulva* spp. seasonal growth dynamics in a temperate location, then the results of this study like represent a less productive time of year for *U. australis*. Considering other environmental variables such as season, temperature, and light intensity are important for building a comprehensive framework from which we can elucidate patterns of ecological relevance from laboratory studies.

Changing pH affected some aspects of *U. australis* physiology (total chlorophyll, $rETR_{max}$, E_k, tissue N, and C:N ratios), and while these changes did not correspond to changes in growth, it cannot be disregard that they may have ecological implications. N-

enriched macroalgae have fewer anti-herbivore defenses and are more palatable (Chan et al. 2012). Indeed, grazing rates have been shown to increase when environmental resources cause increases in primary production (Chan et al. 2012, Falkenberg et al. 2014, Ghedini et al. 2015). This type of trophic compensation can enhance ecosystem stability when there are strong environmental changes such as eutrophication and OA (Ghedini et al. 2015). If grazing pressure increases with decreasing pH due to increased algal palatability, then it is plausible that the abundance of opportunistic algae could decrease in environments where decreasing pH enhances tissue N, but does not permit increased growth rates.

This experiment illustrates the critical role added nutrients play in the stimulation of growth of *Ulva australis* and adds to the substantial body of empirical evidence that nutrient enrichment is a core driver of green tide blooms around the world (Smetacek and Zongone 2013, Teichberg et al. 2010, Liu et al. 2009, Ye et al. 2011). However, I do not predict an increase of *U. australis* biomass due to ocean acidification in the presence or absence of NH_4^+ enrichment. Decreased pH did increase $rETR_{max}$ and tissue N which implies there may be potential for increased growth with decreased pH under a different set of environmental conditions as seen with other experiments (Gordillo et al. 2001, Olischläger et al. 2013, Young and Gobler 2016, Chen et al. 2015, Xu and Gao 2012).

Table 2.1: ANCOVA results for *Ulva australis.*

Variable	*Full Model* [a] pH x NH_4^+ F	p	*Partial Model* [b] pH F	p	NH_4^+ F	p
Relative growth Rates (% day^{-1})	0.00	0.9555	2.65	0.1184	**25.43**	**0.0001**
NH_4^+ uptake rates (µmol g^{-1} FW $hour^{-1}$)	0.04	0.8515	2.90	0.1035	**7.74**	**0.0130**
NH_4^+ Pools (µmol g^{-1} FW)	0.03	0.8733	0.02	0.8939	**14.34**	**0.0012**
Total Chlorophyll (mg g^{-1} FW)	0.00	0.9863	**7.37**	**0.0130**	**10.93**	**0.0034**
$rETR_{max}$	0.04	0.8455	**23.67**	**0.0001**	**33.20**	**0.0000**
E_k (µM photon m^{-2} s^{-1})	3.64	0.0708	**4.38**	**0.0487**	0.22	0.6431
α	2.64	0.1197	0.08	0.7848	**7.25**	**0.0136**
β	2.76	0.1124	0.84	0.3701	**10.11**	**0.0045**
F_v/F_m	0.05	0.4862	**13.79**	**0.001**	**25.71**	**0.0000**
%N	0.23	0.6388	**12.52**	**0.0019**	**56.24**	**0.0000**
%C	0.56	0.4615	1.08	0.3100	0.38	0.5417
C:N	0.18	0.6780	13.23	**0.0015**	**63.47**	**0.0000**

[a]The full model ANCOVA included the interaction term (pH x NH_4^+) to test for differences in the slopes.
[b]If the interaction was non-significant, the partial model ANCOVA including only NH_4^+ (the categorical variable) and the covariate pH (the continuous variable) as factors was used.

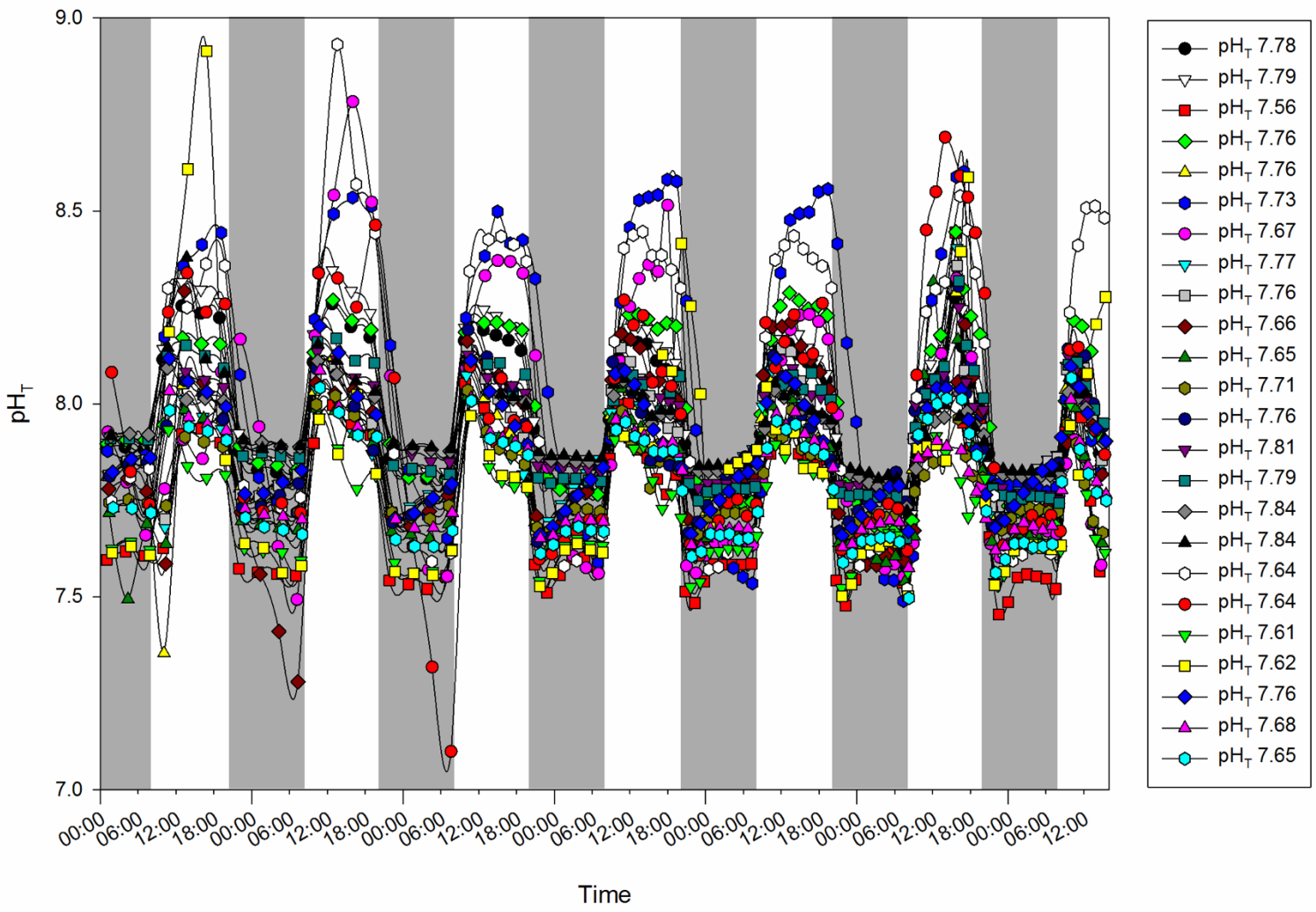

Fig 2.1. Seven day pH_T regime for each pH treatment. The pH monitoring system took pH_T measurements of each *U. australis* growth chambers every 1.5 – 3 hours. Shaded areas of the graph represent dark periods.

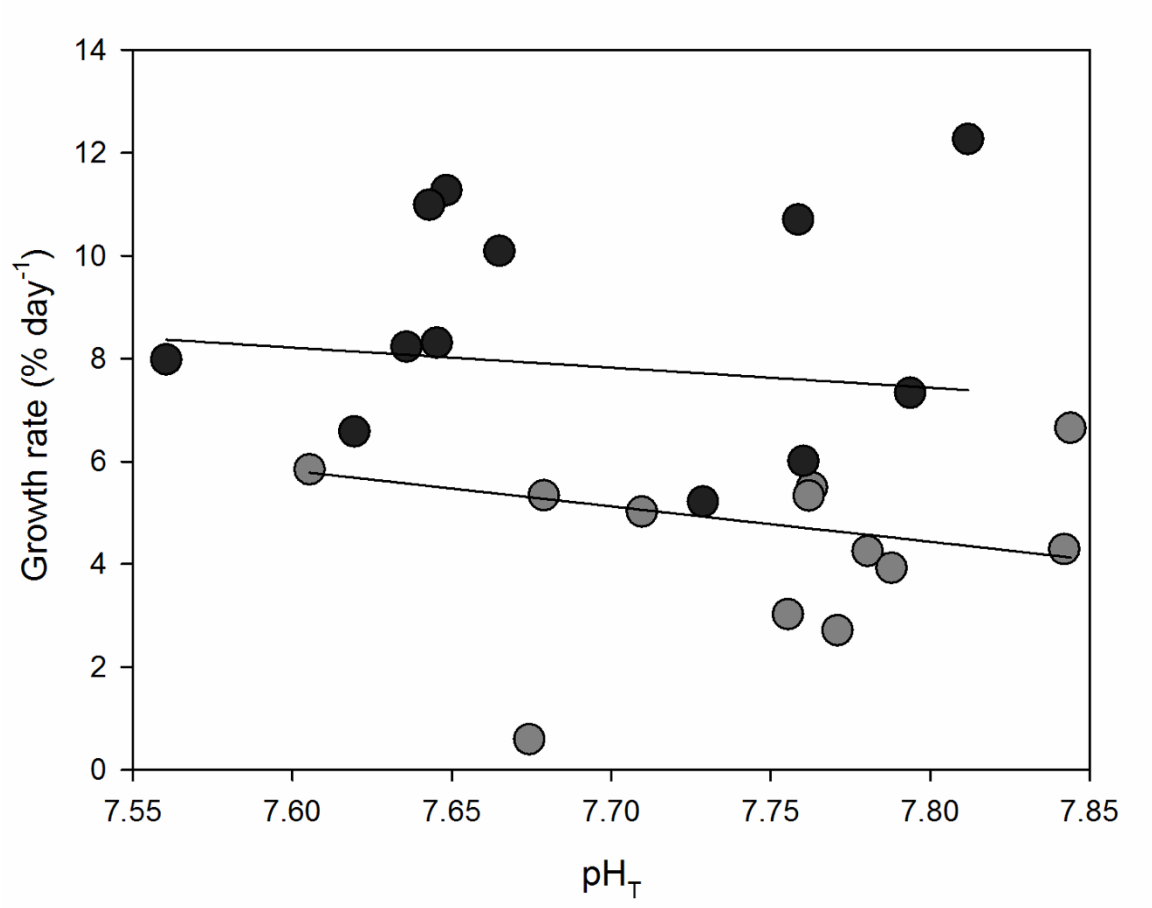

Fig 2.2 Relative growth rates (% day^{-1}) for *Ulva australis* under ambient and enriched NH_4^+ treatments across a range of pH_T. Grey points represent ambient NH_4^+ treatments and black points represent enriched NH_4^+ treatments.

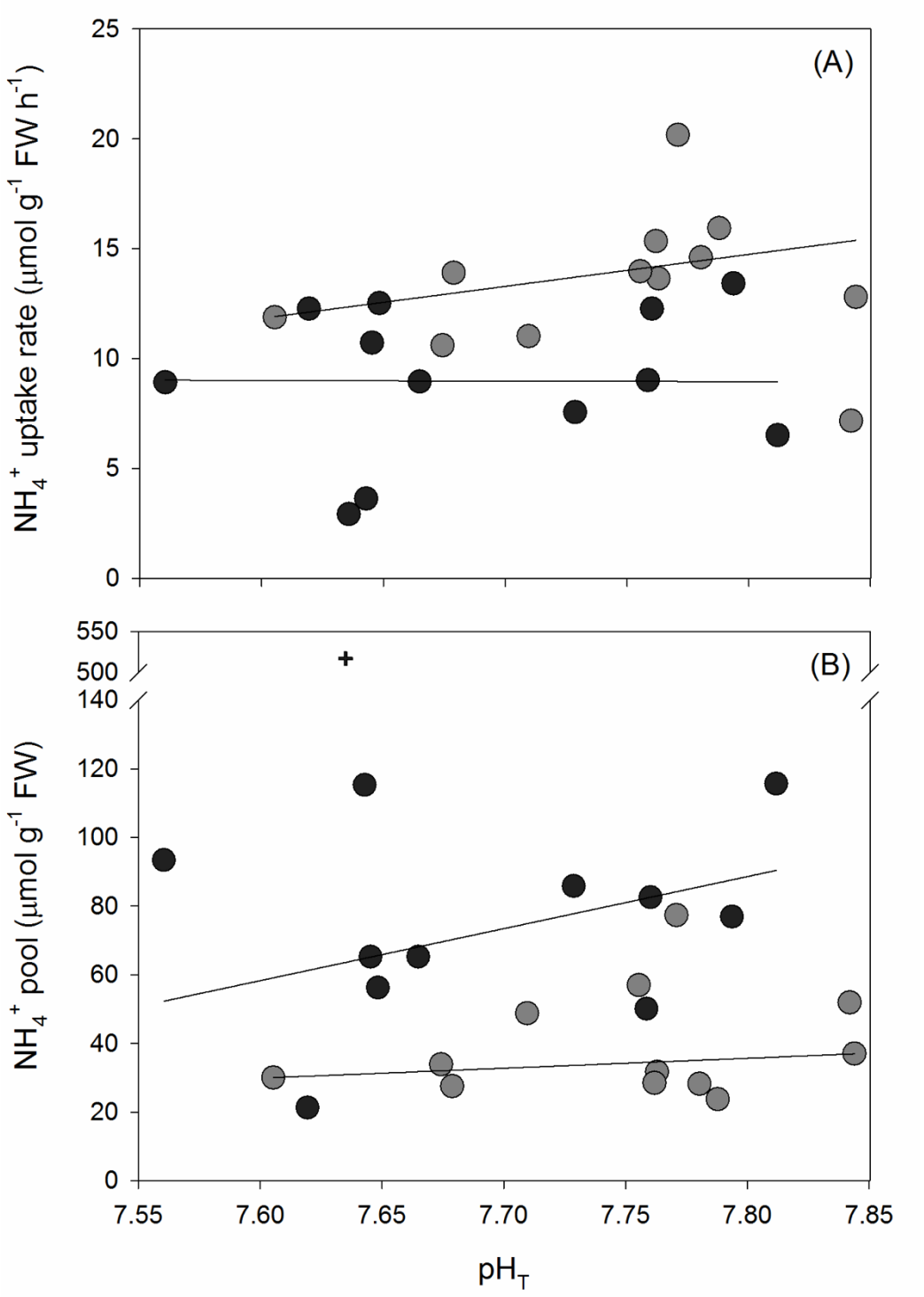

Fig 2.3. (A) NH_4^+ uptake rates (µmol g^{-1} FW $hour^{-1}$) in 20 µM NH4+ seawater for 30 minutes at treatment pH_T and (B) internal NH_4^+ pools (µmol g^{-1} FW) for *Ulva australis* grown under ambient and enriched NH_4^+ treatments across a range of pH_T. Grey points represent ambient NH_4^+ treatments and black points represent enriched NH_4^+ treatments. A plus symbol (+) indicates an outlier which was removed for statistical analysis.

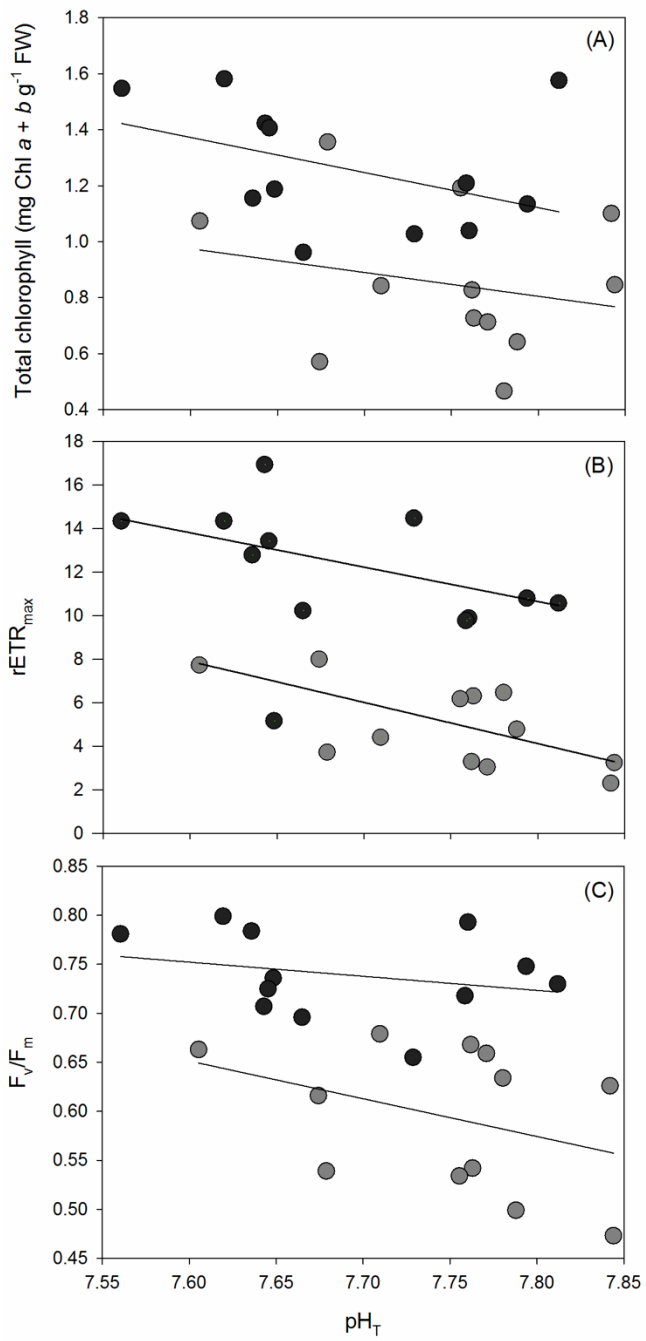

Fig 2.4. (A) Total chlorophyll (mg Chl *a* + *b* g^{-1} FW), (B) $rETR_{max}$ from rapid light curves, and (C) F_v/F_m from rapid light curves for *Ulva australis* grown under ambient and enriched NH_4^+ treatments across a range of pH_T. Grey points represent ambient NH_4^+ treatments and black points represent enriched NH_4^+ treatments.

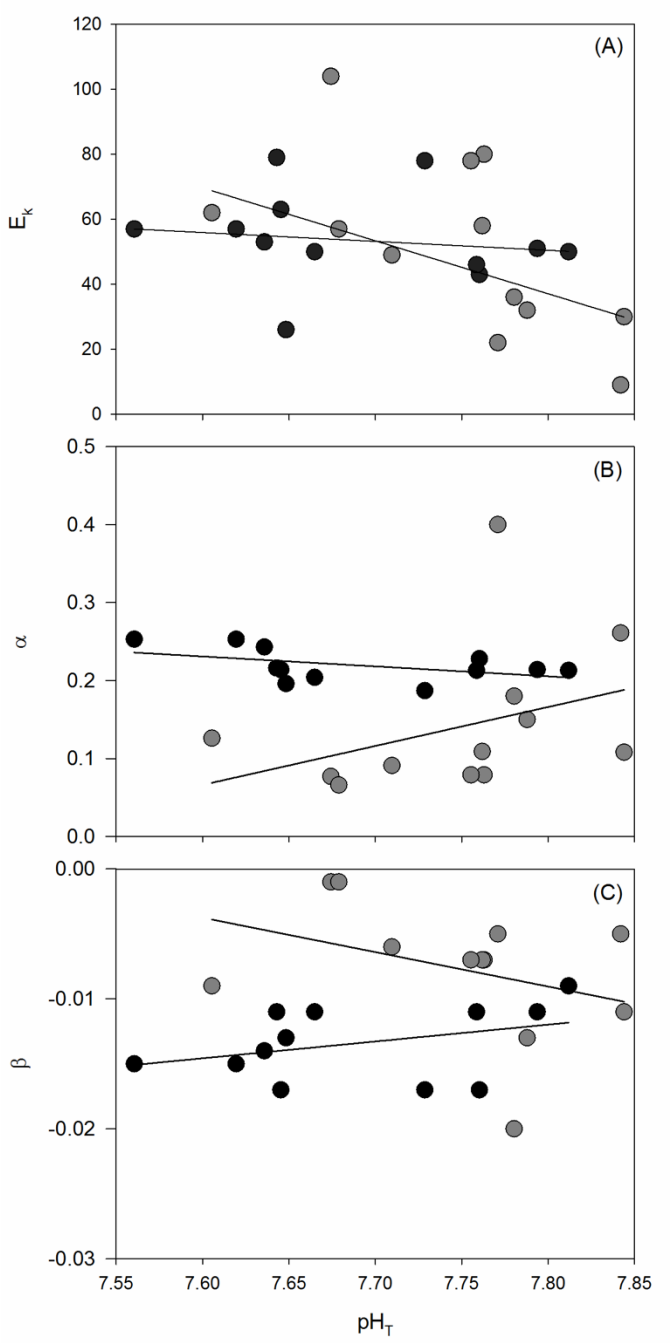

Fig 2.5: (A) Light saturation point (E_k), (B) initial slope of the curve (α), and (C) slope of photoinhibition at high photon flux densities (β) from rapid light curves for *Ulva australis* grown under ambient and enriched NH_4^+ treatments across a range of pH_T. Grey points represent ambient NH_4^+ treatments and black points represent enriched NH_4^+ treatments.

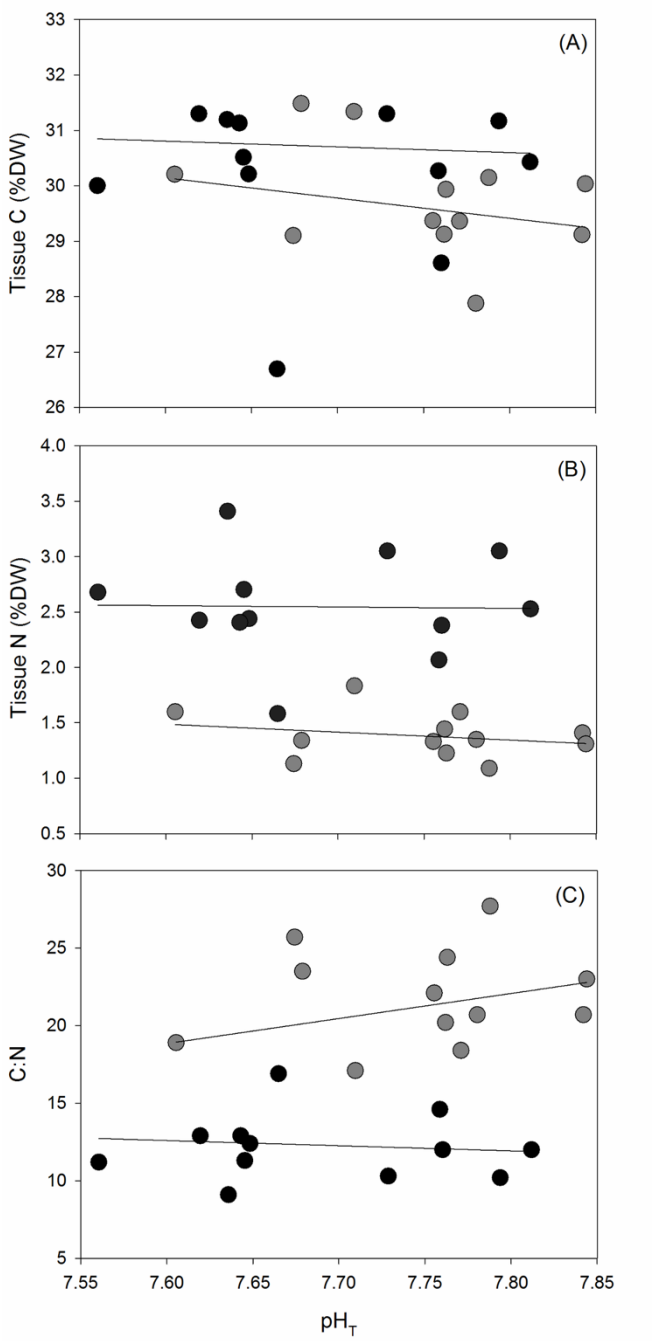

Fig 2.6: (A) Tissue C (%DW), (B) Tissue N (%DW), and (C) C:N ratio of samples of *Ulva australis* under ambient and enriched NH_4^+ treatments across a range of pH_T. Grey points represent ambient NH_4^+ treatments and black points represent enriched NH_4^+ treatments.

CHAPTER 3

The Long-Term Effects of Elevated pCO_2 and Ammonium Enrichment on the Growth, Nutrient, and Photosynthetic Physiology of *Ulva lactuca* (Chlorophyta) in Southern California.

Introduction

Coastal regions are affected by anthropogenic activities due to the close interaction of the sea, land, and atmosphere. Marine macroalgae in coastal regions are subject to many anthropogenically driven changes to the environment including eutrophication and ocean acidification (OA). If historical trends of increased human population density in coastal zones are sustained into the future, increased nutrient supply to estuaries and lagoons is likely (Bricker 2008, Smith 2003, Crosset et al. 2004). Macroalgae in nutrient enriched coastal areas have attributes that contribute to rapid growth rates, such as high nutrient uptake and storage capacities, giving rise to a prolific abundance of macroalgal biomass (Valiela et al. 1997, Smetacek and Zingone 2013). Records of macroalgal blooms began increasing world-wide in the 1960s and 1970s with increased development of industry, agriculture, and urbanization that contribute to increased nitrogen loading in coastal waters (Morand and Briand 1996, Paerl 1997).

Macroalgal growth is typically limited by nitrogen concentrations in seawater (Pedersen et al. 1996). Nitrate (NO_3^-) is the most common and abundant form of dissolved inorganic nitrogen (DIN) in the ocean, and is typically found in concentrations of 0-30 μM in coastal waters while ammonium (NH_4^+) concentrations are typically lower (ca. 3 μM) (Sharp 1983). Most macroalgae favor uptake of NH_4^+, despite its relatively scant availability, because it is less energetically demanding to assimilate than NO_3^- (Miflin and Lea 1976). In coastal areas where sewage output occurs NH_4^+ concentrations

can reach 20 - 25 μM (Sharp 1983). Southern California, one of the most densely populated regions in the United States, has estuaries with the highest nitrogen concentrations in the world (Kennison et al. 2014). The eutrophication of southern Californian estuaries supports the dominance of opportunistic species from the green algal genus *Ulva* (Kennison et al. 2014).

Understanding of how opportunistic algal species, such as *Ulva lactuca,* will respond to the dual environmental changes of OA and NH_4^+ enrichment is currently lacking. OA, caused by increased absorption of CO_2 from the atmosphere into seawater, is expected to change the dissolved inorganic carbon (DIC) chemistry of seawater by increasing pCO_2, HCO_3^-, and H_2CO_3 concentrations and decreasing CO_3^{2-} concentrations and pH (Raven et al. 2005). Macroalgae that exclusively use CO_2 as a carbon source for photosynthesis may respond positively in terms of growth with OA, as they are presently DIC limited (Kübler et al. 1999, Kübler and Dudgeon 2015). However, many macroalgae use carbon concentrating mechanisms (CCMs), which enable the utilization of HCO_3^- and CO_2 from seawater to be used for photosynthesis (Giordano et al. 2005). CCM using algae are thought to be CO_2 saturated at present day pCO_2, but increased diffusive entry of CO_2 with OA, followed by downregulation of CCMs, cause altered carbon metabolic pathways (Raven et al. 1997, Giordano et al. 2005).

Metabolic processes downstream of carbon uptake, such as nitrogen metabolism, are likely to be affected by OA. Carbon metabolism and nitrogen metabolisms are closely linked physiological processes, as products produced from photosynthetic pathways are used for the synthesis of amino acids (Turpin 1991). Furthermore, *Ulva* spp. are known to downregulate CCMs with increased pCO_2 which could lead to an energetic savings that

can be diverted to other physiological process (Raven et al. 2011, Hepburn et al. 2011, Cornwall et al. 2012).

With OA and eutrophication occurring simultaneously on coastlines, I want to understand how a bloom forming green alga, *Ulva lactuca*, from Southern California will respond to several weeks of exposure (ca. 22 days) to a range of pCO_2 and NH_4^+ concentrations. Physiological responses to these conditions were measured including growth, soluble protein and carbohydrate concentrations, nutrient uptake and storage physiology, and photosynthetic physiology. My goals were to determine how much pCO_2, NH_4^+ concentrations, and their interaction affect each physiological response. I used model ranking of standard and conventional multiple regressions to determine which factor or set of factors best represent how *U. lactuca* in Southern California will respond under a range of pCO_2 and NH_4^+ concentrations. The results from this experiment can be applied by marine resource managers to make predictions about *U. lactuca* growth and for guiding policy decisions regarding green macroalgal blooms in the future under various pCO_2 and NH_4^+ scenarios.

Methods

Collection and acclimation

Ulva spp. (morphologically identified as *Ulva lactuca)* was collected from Malibu, CA (34°02'29.0"N 118°34'03.2" W) on May 26, 2016 and July 5, 2016. The thalli were collected from boulders in the intertidal zone. They were placed in re-sealable plastic bags with seawater and transported to the laboratory in a cooler, on ice, within two hours. The thalli were held in aerated autoclaved seawater with PES media (Provasoli 1968) at approximately 17°C under 500 µmol photon m^{-2} s^{-1} light with a 12h:12h light

dark cycle. PES media was supplied every two to three days for a period of ten to eleven days. This allowed the thalli to grow to sizes large enough for the experiment and the PES media assured that the pieces were nutrient replete at the start of the experiment.

Experimental design

The effects of various pCO_2 levels (177 ppm -1376 ppm) on *Ulva lactuca* growth, nutrient, and photosynthetic physiology were evaluated across a range of NH_4^+ concentrations. Each culture tank was aerated with a specific ratio of mixed gases (N_2, O_2, and CO_2) from a mass-flow controlled (MFC) gas mixing system (Qubit Systems, Ontario, Canada). One mixing system delivered mixed gas to four culture chambers each (Fig 3.1). However, the final pCO_2 level differed in each culture tank due to variability in airflow rates, mixing, bubble sizes, and seaweed biomass to sea water volume ratios. Peristaltic pumps delivered autoclaved seawater with modified PES from header tanks to each 3 L culture chamber. Each culture tank was randomly assigned to a MFC gas mixer and NH_4^+ concentration (ambient or high) using a random number generator (RANDOM.org/sequences). The modifications to the PES media included using 1/50 strength nitrate and phosphate and replacement of ferrous ammonium sulfide with iron (III) chloride (see Provasoli 1968). The modification to the PES was necessary to manipulate levels of NH_4^+, while providing nitrogen in the form of NO_3^- to ambient NH_4^+ treatments. Completely removing nitrogen did not allow for long-term culture of *U. lactuca* in preliminary trials. A stock solution of ammonium chloride was added to the NH_4^+ enriched header tanks to a final NH_4^+ concentration of 20 μM. Culture tanks contained a volume of 3 L each, and as new seawater was delivered using peristaltic pumps, wastewater spilled out of tubing at the surface of the water, creating a

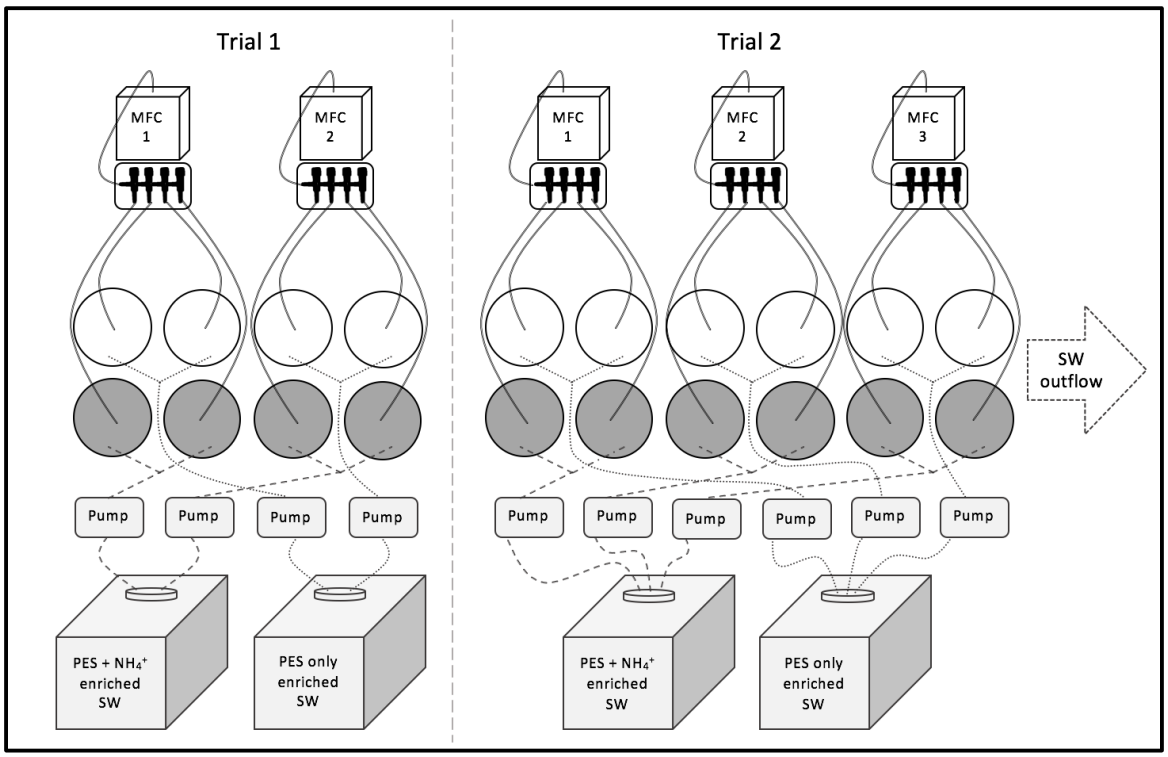

Fig 3.1 Conceptual diagram of experimental set-up. MFCs were connected to N_2, O_2, and CO_2 gases (not shown). Each MFC aerated four culture tanks (circles). Header tanks with 20 L of seawater (SW) with modified PES and either NH_4^+ enriched or not, connected to peristaltic pumps that delivered the SW medium to two culture tanks. Each culture tank was connected to seawater outflow (connections not shown). Connections to MFCs and headers tanks were randomly selected (not shown).

flow-through system. Prior to the start of the experiments, the flow-through system was checked with fluorescent dye to verify that incoming media was well mixed with the seawater in the container before wastewater spilled out. On average, culture tank seawater was completely replaced every 36 hours. The entire culture system was maintained in a cold room with a set temperature of 17°C. Temperature varied throughout the light cycle reaching up to 19.9°C during the light cycle and 15.3°C during the dark cycle. All cultures experienced the same temperatures.

Six *Ulva lactuca* thalli with a total fresh weight of 0.41 ± 0.06 g were grown in culture tanks for approximately three weeks under 500 μmol photon m^{-2} s^{-1} light with a

12h:12h light dark cycle. Using a sterile razor blade, pieces of thalli were removed weekly from the culture chambers to restore seaweed biomass to seawater volume ratio. Photosynthetic characteristics were measured during the last week of each three-week trial and samples for physiological measurements were collected during the last three days of each trial.

pH monitoring and carbonate chemistry

Carbonate chemistry parameters were measured multiple times during each trial using pH and total alkalinity (A_T). A_T samples were collected in 50 mL falcon tubes, stored wrapped in Parafilm at 4°C in the dark, and analyzed within two weeks by potentiometric titration coupled to a pH electrode (Mettler Toledo DGi-115-SC with T5 Rondolino) and thermometer. Most A_T samples were measured on the day of sampling. The performance of the machine was checked with each measurement using certified reference material (CRM) from the Dickson laboratory at the Scripps Oceanographic Institute and the pH electrode was calibrated using TRIS buffer (Dickson et al. 2007). A spectrophotometric technique using m-cresol as an indicator dye was used to determine pH. A_T was calculated using potentiometric titration data and pH using spectrophotometric data in the R-package Seacarb V3.0.14 (Lavigne et al. 2011).

Daily measurements of conductivity, salinity, and temperature were taken with a portable conductivity and salinity meter (Thermo scientific, OrionStar A329) 3 hours after the start of the light cycle. The conductivity meter was calibrated with TRIS buffer. Daily pH monitoring allowed me to adjust mass flow control rates to target set-points as *U. lactuca* thalli grew, increasing the seaweed biomass to sea water volume ratio which in turn, altered pCO_2 levels.

Relative growth rate

The fresh weight of the *Ulva lactuca* thalli was used to determine the relative growth rates (RGRs). Measurements were taken on days 0, 5, 10, and 20, and the RGR was determined for each time period (days 0 – 5, 5 – 10, and 10 – 20). Plants were blotted with tissue paper to remove excess water. The RGR was calculated using the following formula $RGR = \ln((FW_f/FW_i)/\Delta t)*100$. Where FW_i is the initial fresh weight, FW_f is the final fresh weight, and Δt is the time interval. This formula expresses the growth per day as a percentage of the initial weight of the algae in a chamber.

Nitrate reductase activity

An *in vivo* assay of nitrate reductase activity (NRA) was done according to the methods of Thompson and Valiela (1999). First, 5 mL of the incubation medium (equal parts 60 mM KNO_3, 5% propanol, 0.1 M KH_2P0_4 and deionized water; pH 8.0) was flushed with N_2 gas for 2 minutes. *U. lactuca* pieces (0.12 ± 0.07 g) from each treatment were placed in the incubation medium and were flushed again for 2 minutes with N_2 gas. After a 60 min incubation period in the dark at 23°C, 1 mL of the incubation medium was added to a stop buffer (0.5 mL 0.1% napthylethylene diamine, 0.5 mL 5% sulfanilamide, and 2 mL distilled water). Absorbance was measured at 540 nm. Readings were calibrated against a nitrite standard curve. NRA is reported as μmol NO_2^- g FW^{-1} h^{-1}.

Nutrient analysis

20 mL scintillation vials were used to collect water samples throughout the trial. Measurements were taken 1 – 2 times per week (including measurements from the nutrient uptake measurements on day 20). Vials were cleaned with Milli-q water, dried, then soaked in orthophthaldialdehyde (OPA) for 24 – 48 hours to remove NH_4^+ residues

adhered to the glass (Holmes et al. 1999). Then, each vial was rinsed with Milli-q water to remove OPA residue and dried. Samples were collected with new 5 mL pipette tips. First, the vial was rinsed with 10 mL of the seawater sample, then 15 mL was collected and frozen at 0°C until analysis of NH_4^+ and NO_3^- concentrations.

NH_4^+ concentrations in the culture chambers were measured with a fluorometric method using OPA (Holmes et al. 1999) with the suggested modifications of Taylor et al. (2007), which included using an improved method for measuring background fluorescence. The raw fluorescence measurement of a sample was calibrated to a standard curve of an NH_4^+ stock solution using the *standard additions protocol I* of Taylor et al. (2007) which accounts for matrix effects that can alter fluorescence measurements.

NO_3^- concentrations in the culture chambers were determined on samples sent to the University of California, Santa Barbara Marine Science Institute Analytical Lab and were analyzed using a Lachat Instruments flow injection analysis instrument (QuikChem 8000) that determine $NO_3^- + NO_2$ concentrations. In seawater, nitrite (NO_2^-) is typically found in seawater as the oxidized form NO_3^-, therefore the $[NO_3^- + NO_2]$ were a proxy for the $[NO_3^-]$.

Nutrient uptake rates

Uptake rates of NH_4^+ and NO_3^- were measured *in situ* on day twenty of the trials 8 – 10 hours into the light cycle for a period of one hour. The formula for chemostat nutrient uptake by Carmona et al. (1996) was used to determine nutrient uptake rates:

$$\mu mol\ N\ g^{-1}FW\ d^{-1} = \frac{C_{out_i}V + QC_i\Delta t - \frac{Q\left(C_{out_i}C_{out_{i+1}}\right)}{2\Delta t} - C_{out_{i+1}}V}{B\Delta t}$$

where C_i and C_{out} = concentrations of nitrogen in the inflow and the outflow of the system (μM), respectively; V = volume (L), Q = flow rate (L d^{-1}); B= total biomass (g FW L^{-1}), and Δt = time in days.

CN analyses and carbon stable isotope ratios

Samples for tissue organic carbon and nitrogen content, tissue stable carbon isotopes, and seawater carbon stable isotopes were collected on day 20. Tissue samples were dried for 24 hours at 60°C. Dried samples were prepared for analysis by homogenizing samples using a metal laboratory scoop, cleaned with ethanol between each sample, which resulted in a fine power. Then, approximately 3 mg of the *Ulva lactuca* tissue powder was measured, using an analytical balance (Mettler Toledo XP205), into a tin capsule and carefully enclosed with cleaned forceps. The tin capsules were put into 96-well trays and sent to the University of California, Davis Stable Isotope Facility (UCD-SIF). The samples were analyzed for $\delta^{15}N$ and $\delta^{13}C$ using the elemental analysis – isotope ratio mass spectrometry technique, which also provides results for tissue C and N content.

Samples for $\delta^{13}C$ of DIC in the seawater were stored in 20 mL glass vials with cone lids to exclude air from samples. Samples were stored at room temperature in low light until prepared for analysis using the exetainer gas evolution technique for DIC (Li et al. 2007). Then, the samples were sent to the UCD-SIF for analysis using the GasBench – isotope ratio mass spectrometry technique. The discrimination of carbon stable isotopes (Δ) was determined by correcting the tissue $\delta^{13}C$ for the $\delta^{13}C$ of the source gas using the formula $\Delta = (\delta^{13}C_{source} - \delta^{13}C_{plant})/ (1 + \delta^{13}C_{plant})$. Furthermore, Δ was used for

determining if CCMs respond to increasing pCO_2 and NH_4^+ enrichment (Raven et al. 2002).

Internal soluble nitrogen pools

Internal NH_4^+ and NO_3^- pools were measured using the boiling water method (Hurd et al. 1996). One piece (0.04 ± 0.02 g FW) from each treatment was rinsed with deionized water to remove salt and nutrients on the surface. The pieces were placed in test tubes with 15 mL of deionized water and placed in a boiling water bath for 40 minutes. The water was decanted and analyzed for NH_4^+ and NO_3^-. The process was repeated in triplicate to remove all internal N pools.

Soluble protein and carbohydrates

Pieces of *Ulva lactuca* tissue (0.04 g FW) were ground in a mortar and pestle in 2 mL of a β-mercaptoethanol buffer, pH 7.5 and stored at 4°C for up to 72 hours. The extract was centrifuged at 16,000 g for 5 minutes. Soluble proteins and carbohydrates were determined spectrophotometrically (Milton Roy Spectronic Genesys 5) using the supernatant fraction. Soluble proteins were determined according to Bradford (1976) and soluble carbohydrates using the phenol-sulfuric acid method according to Kochert (1978).

Photosynthetic rates

Photosynthetic O_2 evolution rates were measured using the Qubit systems O_2 electrode in a water jacketed cuvette connected to a laptop using a LabPro™ interface. Small pieces of *Ulva lactuca* (1 – 2 cm^2) were cut from thalli at least one hour prior to measurements. The pieces were placed in 20 mL of culture water at 16°C in a 2 cm^2 mesh bag which held the pieces at a 90° angle to the Qubit LED light source. A photosynthesis-

irradiance (P-I) curve was generated using various photon flux densities from 0 – 700 μmol photons m^{-2} s^{-1} for 200 seconds each, following a 200 second dark period to measure dark respiration rate. The maximum photosynthetic rate (P_{max}), light saturation point (I_k), and the initial slope of the P-I curve (α), were determined from the P-I curves.

Data analysis

pCO_2 and NH_4^+ levels

Each culture was designated a specific pCO_2 and NH_4^+ concentration which was used for all analyses. The pCO_2 treatment of each culture chamber was denoted by the average pCO_2 over the entire trial. Instantaneous measurements of nutrients in water samples are not suitable indications of the bioavailability of nitrogen to *Ulva* spp. (Barr 2007, Fong et al. 1998). Therefore, the NH_4^+ concentration of each culture chamber was determined by the average difference between header tank NH_4^+ concentrations and culture chamber NH_4^+ concentrations, assuming that difference was the NH_4^+ removed by the algae.

Model selection

Generalized linear mixed models (GLMM) were used to evaluate the physiological responses of *Ulva lactuca* to a range of pCO_2 and NH_4^+ concentrations (NH_4^+ henceforth). pCO_2, NH_4^+, and the interaction were evaluated as fixed effects, and trial as a random effect. Models that included NH_4^+ and/or pCO_2 as a random effect across trials with correlated, or uncorrelated, slopes and intercepts were also evaluated. The fixed and random factors were used to develop a set of 23 candidate models *a priori.* Variation due to random effects were described by the variance components. The data were evaluated for normality using a Shapiro-Wilk test and were transformed, if

necessary. Further, the data were standardized using z-scores in order to assess the effects of pCO_2 and NH_4^+ using standardized regression coefficients. Akaike's Information Criterion, corrected for small-sample bias (AIC_c) was used to rank the candidate models (Anderson 2008). Models with a $\Delta AIC_c < 3$ were considered as models that best represent full reality given the present data set.

Standardized effect size

The z-score standardized effect sizes show how far each factor drives a physiological response from the mean. Effect sizes were calculated using weighted model-averaged parameter estimates for the fixed effects from the aforementioned analysis. Information from the entire *a priori* model set was used to determine effects sizes, so as not to lose information from lower ranked models (Anderson 2008).

Conventional regression coefficients

In a manner similar to the aforementioned analyses, the unstandardized, untransformed data were analyzed using GLMM. Conventional regression coefficients were calculated using weighted model-averaged parameter estimates using the same *a priori* developed model set. Then, the data were used to make predictions using the linear expression $y = \beta_0 + \beta_1 * x_1 + \beta_2 * x_2 + \beta_3 * (x_1 * x_2)$, where $x_1 = pCO_2$ and $x_2 = NH_4^+$. Mesh plots of the responses were overlaid with the data from the experiment. Data analysis was done in R using the lmer4 and AICcmodavg packages (Mazerolle 2013).

Results

After day 5, RGRs of *Ulva lactuca* were not affected by pCO_2, NH_4^+, or their interaction, but during days 0 – 5 there was a positive interaction on RGRs (Fig 3.2). This positive interaction was supported by the best models (Table 3.1). During days 0 – 5 and

days 5 – 10, variance components showed that > 90% of the variance in the data could be contributed to differences in responses between trials. Conventional regression coefficients show that the relative growth rates decreased over time and that the interaction of pCO_2 and NH_4^+ could cause relatively increased growth rates at high pCO_2 and NH_4^+ concentrations (Fig 3.3).

Tissue NH_4^+ and NO_3^- pools were negatively affected by pCO_2 enrichment, but the 95% CI overlapped zero so this is considered a weak effect. The best models indicate that pCO_2 should be included as a predictor in models for both types of nitrogen storage (Fig 3.2 and Table 3.1). Conventional regressions show that the NH_4^+ pools were less concentrated in *Ulva lactuca* than NO_3^- pools and that the decrease in concentration with increasing pCO_2 was greater for NO_3^- pools than NH_4^+ pools (Fig 3.4A, 3.4C). Variance in the data could be attributed to the random effect of trial for NO_3^- and NH_4^+ pools, but this depended on the model used and ranged from 13.54 – 51.11% (Table 3.1).

There was a weak positive effect of NH_4^+ net depletion on *in situ* NH_4^+ uptake rates, but the 95% CI overlapped zero (Fig 3.2). Despite the low confidence in the positive effect of *in situ* NH_4^+ uptake rates being different from zero, mesh plots derived from conventional regressions showed that *in situ* NH_4^+ uptake rates increased as NH_4^+ increased (Fig 3.4B). The best models for *in situ* NH_4^+ uptake rates showed that NH_4^+ is a good predictor of *in situ* NH_4^+ uptake rates (Table 3.2). The set of best models indicated that as a random factor NH_4^+ concentration contributed ca. 30% of the variation in *in situ* NH_4^+ uptake rates between trials, and 33.71 – 47.93% of the variation was due to trial alone (Table 3.1).

The effect of NH_4^+ concentrations on *in situ* NO_3^- uptake rates was also weak with a 95% CI overlapping zero, but negative, where increasing NH_4^+ concentrations decreased NO_3^- uptake rates (Fig. 3.2). Further, the mesh plots of conventional regressions did not show an effect on NH_4^+ concentration on *in situ* NO_3^- uptake rates at low pCO_2. However, at high pCO_2 the *in situ* NO_3^- uptake increased with NH_4^+ enrichment indicating an interactive effect (Fig 3.4D). The interaction was positive, based on standardized effect sizes and predictive mesh plots using conventional regression coefficients (Fig 3.2 and Fig 3.4D), but was not included as a good predictor of *in situ* NO_3^- uptake rates (Table 3.1). So despite the presence of an interaction, NH_4^+ concentration is the best predictor for NO_3^- uptake rates based on the data from this experiment. Zero percent of the variance was attributed to the random effect of trial, so the effect of NH_4^+ and pCO_2 concentrations on *in situ* NO_3^- uptake rates did not change across trials. The effects of pCO_2 and NH_4^+ or the interaction on NRA (Fig 3.2) and variance components indicate that this did not vary across trials (Table 3.1).

Soluble protein concentrations were not affected by pCO_2, but the effect of NH_4^+ enrichment was positive (Fig 3.2). The random effect of trial contributed to approximately 60% of the variation in the data and NH_4^+ concentration was the best predictor of protein concentrations in *U. lactuca* (Table 3.1). Soluble carbohydrate concentrations were not affected by pCO_2, NH_4^+, or their interaction (Fig 3.2).

P_{max} was negatively affected by pCO_2 and there was a weak positive effect of NH_4^+ concentration on P_{max}, but the 95% CI overlapped zero (Fig 3.2). These effects were substantiated by mesh plots of P_{max} from conventional regressions (Fig 3.5C). The best factors for predicting P_{max} included both pCO_2 and NH_4^+, but not the interaction

between them. The random effect of trial contributed 0-4.71% of the variation in P_{max}, so the effects of pCO_2 and NH_4^+ were consistent across trials. There was a weak negative affect of pCO_2 on α, where the 95% CI overlapped zero (Fig 3.2), and variance components from model selection showed that variance due to trial ranged from 0.88 – 28.12% (Table 3.1). Conventional coefficients for α showed that that there was no effect of NH_4^+ or the interaction on α, but the coefficient for pCO_2 was -0.88 (Table 3.2).

The effects of pCO_2, NH_4^+, and their interaction were weak (95% CI overlapping 0), but positive, for I_k. Variance components from the best models indicate that 46.58 – 62.24% of the variation can be attributed to variation between trials (Table 3.1). The best models show that the factors pCO_2 or NH_4^+ should be included as predictors for I_k (Table 3.1). Weighted, model-averaged estimates of conventional regression coefficients substantiate the weak positive effect of pCO_2, NH_4^+, and the interaction on I_k. There was a weak negative effect of pCO_2 on the dark respiration rate (95% CI overlapped zero), while there was no detectable effect of NH_4^+ and the interaction. Responses of *U. lactuca* dark respiration rates did not vary substantially trial to trial according to the variance components of the most supported models (Table 3.1). The best models show that the factors pCO_2 or NH_4^+ should be included as predictors for dark respiration rates (Table 3.1). There was no effect of pCO_2, NH_4^+ or the interaction on Chl *a* + *b* (Fig. 3.2). Nevertheless, the best models indicated that $NH_4^+$was the best predictor for Chl *a* + *b* and that 47.87 – 53.60% of the variation in the data was due to difference between trials (Table 3.1).

NH_4^+ concentrations were the best predictors for tissue C, tissue N, and C:N ratios (Table 3.1). However, pCO_2 and the interaction did not have detectable effects on tissue

C and N or the C:N ratio (Fig. 3.2). The effects of NH_4^+ on tissue C, tissue N, and the C:N ratio were relatively large, but weak (95% CI overlapping zero); tissue C and N were positively affected, and the C:N ratio was negatively affected (Table 3.1). The variance components from the best models showed that the effect of NH_4^+ contributed to 53% of the variability across trials in tissue C and 79% of the variation in tissue N and the C:N ratio. This led to the large 95% CI, making estimates of the effect size of NH_4^+ concentrations uncertain in this case (Table 3.1).

$\delta^{15}N$ was negatively affected by pCO_2 and NH_4^+ enrichment, but not the interaction (Fig 3.2). The best models indicate that pCO_2 and NH_4^+ were good predictors for $\delta^{15}N$ in this experiment and 30.54 – 46.78% of the variation could be attributed to variation between trials (Table 3.1). The mesh plots derived from model-averaged conventional regression coefficients estimates show that as pCO_2 and NH_4^+ concentrations increase, the $\delta^{15}N$ signature decreases (Fig 3.5B). There was no detectable effect of pCO_2 and NH_4^+ concentrations on $\Delta^{13}C$, but there was a negative effect with the interaction (Fig 3.2). The best models indicated that the factors NH_4^+ and pCO_2 were suitable for making predictions, but not the interaction factor (Table 3.1) and the weighted model-average conventional regression coefficients estimates show that the interaction is small (<0.01) but significant (Table 3.2). The mesh plot substantiates the interaction by showing that Δ decreased only when pCO_2 and NH_4^+ concentrations were high (Fig 3.5D).

Discussion

Green macroalgal blooms are common on southern Californian coasts where nutrient enrichment is high due to dense human populations (Kennison et al. 2014). With

OA, fleshy macroalgae are predicted to benefit in terms of growth rate (Kroeker et al. 2013), and there is concern that simultaneous OA and eutrophication will have additive or interactive effects which increase growth rates of opportunistic green algae and the occurrence of green tide blooms. Previous studies that examined the effects of OA and eutrophication on *Ulva* spp. occurred over periods of 7 – 10 days, which precludes the determination of longer-term effects and the occurrence of acclimation (Gordillo et al. 2001, Gordillo et al. 2003, Young and Gobler 2016, Reidenbach Chapter 2). The results of this experiment show that with respect to growth, there are short-term, acute positive effects of NH_4^+ and pCO_2 enrichment and *Ulva lactuca* acclimate to OA and eutrophication through longer-term exposure.

When pCO_2 and NH_4^+ enrichment occurred simultaneously, the RGR of *Ulva lactuca* was positively affected by the interaction during days 0 – 5. Further, I found that the RGR was not affected by the interaction on days 5 – 10 and 10 – 20, suggesting that *Ulva lactuca* had acclimated to combined pCO_2 and NH_4^+ enrichment, returning to average growth rates by the 10^{th} day. The RGR was not affected by pCO_2 or NH_4^+ enrichment alone throughout the experiment. First, this demonstrates that OA alone did not influence the RGR of *Ulva lactuca*. This has been found with other OA experiments on a variety of macroalgal species from tropical and temperate environments (Reidenbach Chapter 2, Israel and Hophy 2002, Bender-Champ et al. 2017). Second, despite the fact that *Ulva* spp. are among the most opportunistic algal species (Littler and Littler 1980) and typically demonstrate higher growth rates with nitrogen enrichment (Fong et al. 2004) it was surprising that NH_4^+ enrichment did not have an effect on the RGR. However, the nutrient history of macroalgae plays an important role in determining

responses to nutrient enrichment (Fujita 1985, Naldi and Viaroli 2002, Fong et al. 2003, Kennison et al. 2011). For example, the growth rate of *U. lactuca* in response to NO_3^- or NH_4^+ enrichment was greater, relative to control treatments, from sites with relatively low DIN in the water column when compared to algae from eutrophic sites (Teichberg et al. 2008). Here, this response, or lack thereof, was likely caused by the initial N-replete nutrient status of the algae, which were collected from a eutrophic environment and then kept under nutrient enriched conditions for ten to eleven days prior to the experiment.

Evidence to demonstrate the connection between carbon and nitrogen metabolism comes from the $\delta^{15}N$ results. Under NH_4^+ enrichment the $\delta^{15}N$ decreased reflecting the stable isotope signature of the NH_4Cl (Sigma A9434) used to enrich the medium which was incorporated into algal tissue with growth under NH_4^+ enrichment. Further, the $\delta^{15}N$ was affected by pCO_2 indicating that the incorporation of NH_4^+ was increased with pCO_2 enrichment throughout the experiment. NH_4^+ enrichment increased protein concentrations, but I did not detect any strong effects of NH_4^+ enrichment on N pools or uptake rates, but the direction of the effect sizes was as expected. NH_4^+ pools and *in situ* uptake rates increased and NO_3^- uptake rates decreased with NH_4^+ enrichment. However, with 95% CI overlapping zero, the effects were weak and it cannot be determined if this was due to the initial N-replete nutrient status, small sample sizes, or a combination of both.

NO_3^- pools in plants indicate the occurrence of a surplus of inorganic N that has yet to be reduced to organic N (Stitt and Krapp 1999). pCO_2 had a weak negative effect on NO_3^- and NH_4^+ pools in this experiment indicating OA may stimulate N assimilation in *Ulva lactuca*, but the 95% CI overlapped zero. However, this effect has been reported

with *Pyropia haitanensis* (Liu and Zou 2015), *Ulva rigida* (Gordillo et al. 2001), and *Zostera noltii* (Alexandre 2012). The relationship between pCO_2 enrichment and decreased NO_3^- pools are typically explained by an association with increased carbon skeleton availability via increased photosynthetic rates or a reduction in carbohydrate storage (Turpin 1991, Stitt and Krapp 1999), but neither NRA nor NO_3^- uptake were affected by pCO_2. However, there was a positive interactive effect on NO_3^- uptake where the combination of increased nutrients (NH_4^+) and pCO_2 stimulated NO_3^- uptake. pCO_2 and NO_3^- enrichment increased NRA in *Ulva ridgida* (Gordillo et al. 2001), and we now know that the provision of excess NH_4^+ under pCO_2 enrichment could lead to increased NO_3^- uptake even though NH_4^+ is typically known to suppress NO_3^- assimilation (McGlathery et al. 1996). NH_4^+ has been shown to increase anaplerotic reactions, which replenish tricarboxylic acid (TCA) cycle intermediates, and drive amino acid synthesis in *Selenastrum minutum* (Vanlerberghe et al. 1990). This, coupled to increased carbon availability, may lead to downstream increases in NO_3^- uptake as seen here. Increased nitrogen and pCO_2 stimulating the energetic process of NO_3^- metabolism (Turpin 1991) would lead to increased growth as seen in days 0 – 5.

P_{max} decreased with pCO_2, agreeing with the findings of Björk et al. (1993), Gordillo et al. (2001), and Gao et al. (2016) with several *Ulva* species. NH_4^+ did not play a role in mediating this effect, as there was no effect of the interaction on P_{max}. Two processes can result in a down regulation or loss of CCMs: increased diffusion of pCO_2 and low light intensities (Raven et al. 2011, Hepburn et al. 2011, Cornwall et al. 2012). However, under high light intensities, the demand for photosynthesis increases and CCMs are required to keep up with this demand (Hepburn et al. 2011). Gao et al. (2016)

found that *U. linza* acclimated to high-CO_2 conditions for three weeks downregulated CCMs and had decreased photosynthetic rates upon exposure to high light intensities. Here, *U. lactuca* was acclimated to high light intensities for three weeks under experimental growth conditions and demonstrated decreased P_{max} when grown under increased pCO_2 and CCMs were not affected by pCO_2 alone. Under ambient NH_4^+, high CO_2 conditions there was no alteration of CCM pathways as shown by Δ, indicating that CCMs continued to operate. In this case, CCMs were needed to keep up with photosynthetic demand and to compensate for increased photodamage and inability to photoacclimate under high light intensities as seen with *U. linza* grown under increased pCO_2 as indicated by increased non-photosynthetic quenching (Gao et al. 2016). Addition of NH_4^+ can alleviate photodamaging processes and allow for normal cellular function under high light intensities (Henley et al. 1991).

Furthermore, the interaction of pCO_2 and NH_4^+ decreased Δ which is interpreted as an alteration of CCM pathways (Raven et al. 2002). Under pCO_2 and NH_4^+ enrichment, CCMs may have been downregulated which can result in an energetic savings which, here, were likely invested into other metabolic processes such as NO_3^- assimilation. However, this comes with a tradeoff: when CCMs are downregulated, there is a limit to maximum photosynthetic rates stimulated by pCO_2 availability in the water column which can normally be overcome when CCMs are fully operational. The results from this study indicate that *Ulva* spp. rates of photosynthesis may be negatively affected by OA under high light conditions.

This experiment is the first to demonstrate longer-term effects of OA and NH_4^+ enrichment on the growth and physiology of *Ulva lactuca*. Further, the results of this

research provide useful information to guide predictions about *U. lactuca* growth and production under future OA and eutrophication scenarios. However, this should only be applied to the southern California region from which they were collected, as algal environmental history plays a role in its responses. I found that while OA and eutrophication may have synergistic effects on growth rates as seen in other studies, this effect was only seen during short-term exposure. After acclimation to longer-term exposure, there is no interaction and OA does not benefit *U. lactuca* in terms of growth. Further, increased pCO_2 under experimental high light intensities was found to be detrimental to maximum photosynthetic rates. This study was the first to demonstrate that NH_4^+ enrichment interacts with pCO_2 enrichment to increase NO_3^- uptake, as found with NO_3^- enrichment. This could lead to increased initial growth rates upon exposure to either OA or NH_4^+, so studies should be done to investigate how pulses of nitrogen affect *Ulva* spp. growth with OA, especially with respect to bloom initiation. *U. lactuca* in southern California is unlikely to experience changes in growth and physiology with OA in already eutrophic environments, which speaks to the resiliency and adaptability of this opportunistic algal species.

Table 3.1: Summary of most supported models ($\Delta AIC_c \leq 3$) and variance components.
Number of parameters (K), Akaike Information Criterion corrected (AICc), AIC_{ci} – AIC_{Cmin}(ΔAICc), Model weight (W_i), evidence ratio (ER).

						Variance Components (%)		
Best Models	**K**	**AICc**	**ΔAICc**	**W_i**	**ER**	**Trial**	**[NH4+]**	**e**
RGR Days 0 – 5 (% day^{-1})								
NH_4^++(NH_4^+|Trial)	6	34.21	0	0.24	1.00	90.96	4.64	4.40
NH_4^++(1|Trial)	4	34.49	0.28	0.21	1.14	92.94		7.06
NH_4^++(NH_4^+||Trial)	5	35.1	0.89	0.15	1.60	91.15	4.17	4.68
1+(1|Trial)	3	35.11	0.9	0.15	1.60	91.42		8.58
CO_2+ NH_4^++ CO_2*NH_4^++(1|Trial)	6	35.39	1.19	0.13	1.85	94.84		5.16
RGR Days 5 – 10 (% day^{-1})								
1+(1|Trial)	3	57.99	0	0.51	1.00	91.42		8.58
CO_2+(1|Trial)	4	60.14	2.15	0.17	3.00	90.95		9.05
NH_4^++(1|Trial)	4	60.94	2.95	0.12	4.25	92.94		7.06
RGR Days 10 – 20 (% day^{-1})								
1+(1|Trial)	3	57.54	0	0.52	1.00	58.38		41.62
NH_4^++(1|Trial)	4	60.43	2.89	0.12	4.33	58.38		41.62
Soluble Carbohydrates (mg ml^{-1} g^{-1} FW)								
NH_4^++(NH_4^+Trial)	6	55.3	0	0.33	1.00	58.64	25.27	16.09
1+(1|Trial)	3	55.62	0.32	0.28	1.18	64.77		35.23
NH_4^++(NH_4^+||Trial)	5	56.58	1.28	0.18	1.83	57.20	25.93	16.87
CO_2+(1|Trial)	4	57.78	2.48	0.1	3.30	58.81		41.19
Soluble Proteins (mg ml^{-1} g^{-1} FW)								
NH_4^++(1|Trial)	4	54.1	0	0.6	1.00	59.64		40.36
NH_4^+ Pools (µM g^{-1} FW)								
1+(1|Trial)	3	63.2	0	0.37	1.00	13.53		86.47
CO_2+(1|Trial)	4	64.3	1.1	0.22	1.68	40.50		59.50
NH_4^++(1|Trial)	4	64.56	1.36	0.19	1.95	20.08		79.92
CO_2+ NH_4^++(1|Trial)	5	65.65	2.45	0.11	3.36	46.32		53.68
NO_3^- Pools (µM g^{-1} FW)								
CO_2+(1|Trial)	4	58.96	0	0.39	1.00	37.12		62.88
1+(1|Trial)	3	59.23	0.27	0.34	1.15	51.11		48.89
NH_4^+ Uptake Rates (µM g^{-1} FW h^{-1})								
NH_4^++(1|Trial)	4	58.31	0	0.26	1.00	47.93		52.07
NH_4^++(NH_4^+|Trial)	6	58.5	0.19	0.24	1.08	44.69	30.84	24.47
NH_4^++(NH_4^+||Trial)	5	58.63	0.33	0.22	1.18	44.02	29.33	26.64
1+(1|Trial)	3	59.22	0.92	0.17	1.53	33.71		66.29
NO_3^- uptake rates (µM g^{-1} FW h^{-1})								
1+(1|Experiment)	3	52.37	0	0.5	1.00	0		100
NH_4^++(1|Experiment)	4	53.68	1.31	0.26	1.92	0		100

Table 3.1: Continued.

Best Models	K	AICc	ΔAICc	Wi	ER	Variance Components (%) Trial	[NH4+]	e
NRA (µM NO_2^- g FW^{-1} h^{-1})								
1+(1|Experiment)	3	63.23	0	0.63	1.00	0		100
NH_4^++(1|Experiment)	4	66.01	2.78	0.16	3.94	0		100
Chl *a* + *b* (mg g^{-1} FW)								
1+(1|Trial)	3	58.7	0	0.38	1.00	53.60		46.40
NH_4^++(1|Trial)	4	59.89	1.19	0.21	1.81	51.71		48.29
NH_4^++(NH_4^+||Trial)	5	61.64	2.94	0.09	4.22	47.87	20.52	31.60
P_{max} (µM O_2 g FW^{-1} min^{-1})								
CO_2+ NH_4^++(1|Trial)	5	59.99	0	0.39	1.00	0		100
NH_4^++(1|Trial)	4	60.94	0.95	0.24	1.63	4.71		95.29
SCO_2+(1|Trial)	4	62.03	2.03	0.14	2.79	0		100
α								
1+(1|Trial)	3	63.23	0	0.5	1.00	0.88		99.12
CO_2+(1|Trial)	4	64.55	1.32	0.26	1.92	28.12		71.88
NH_4^++(1|Trial)	4	66.17	2.94	0.11	4.55	2.11		97.89
I_k (µmol photon m^{-2} s^{-1})								
1+(1|Trial)	3	59.65	0	0.41	1.00	48.97		51.03
NH_4^++(1|Trial)	4	61.16	1.51	0.19	2.16	46.58		53.42
CO_2+(1|Trial)	4	61.3	1.64	0.18	2.28	62.24		37.76
Respiration (µM O_2 g FW^{-1} min^{-1})								
1+(1|Trial)	3	63.23	0	0.39	1.00	0		100
CO_2+(1|Trial)	4	63.82	0.58	0.29	1.34	5.00		95.00
NH_4^++(1|Trial)	4	65.24	2.01	0.14	2.79	0		100
Tissue C (µg mg^{-1} FW)								
NH_4^++(NH_4^+||Trial)	5	58.66	0	0.44	1.00	17.29	53.38	29.33
NH_4^++(NH_4^+|Trial)	6	58.95	0.29	0.38	1.16	19.32	53.56	27.12
Tissue N(µg mg^{-1} FW)								
NH_4^++(NH_4^+||Trial)	5	48.38	0	0.76	1.00	1.35	79.84	18.82
NH_4^++(1|Trial)	6	50.86	2.48	0.22	7.82	3.24	79.28	17.48
C:N								
NH_4^++(NH_4^+||Trial)	5	48.9	0	0.81	1.00	1.85	79.16	19.00
$\delta^{15}N$ (‰)								
CO_2+ NH_4^++(1|Trial)	5	52.22	0	0.47	1.00	30.54		69.46
NH_4^++(1|Trial)	4	53	0.78	0.32	1.47	46.78		53.22
Δ								
1+(1|Trial)	3	61.56	0	0.51	1.00	36.48		63.52
NH_4^++(1|Trial)	4	63.58	2.02	0.19	2.68	33.30		66.70
CO_2+(1|Trial)	4	64.19	2.63	0.14	3.64	47.54		52.46

Table 3.2 Weighted, model-averaged estimates of conventional regression coefficients and standard error of mean (SEM) for each experimental parameter. Intercept (β_0), pCO_2 (β_1), $[NH_4^+]$ (β_2), pCO_2*$[NH_4^+]$ (β_3).

	β0	SEM	β1	SEM	β2	SEM	β3	SEM
RGR Days 0 – 5	29.23	5.14	-5.26	24.68	0.22	0.17	0.06	0.02
RGR Days 5 – 10	25.80	2.98	-24.33	28.13	0.04	0.16	0.05	0.03
RGR Days 10 – 20	14.30	3.05	36.38	58.27	0.01	0.29	0.02	0.05
Soluble Carbohydrate	25.41	8.75	49.17	50.71	-0.18	0.46	-0.02	0.07
Soluble Protein	1.10	0.58	-1.89	4.74	0.06	0.02	0.01	0.01
NH_4^+ Pools	0.62	0.20	-3.45	1.94	0.01	0.01	0.00	0.00
NO_3^- Pools	12.95	3.84	-106.28	43.40	-0.01	0.15	-0.02	0.04
NH_4^+ Uptake	0.06	2.22	20.12	38.44	0.41	0.29	0.02	0.04
NO_3^- Uptake	3.76	1.43	-5.75	14.51	-0.11	0.07	0.05	0.02
NRA	65.11	11.40	-23.65	200.33	0.57	0.96	0.28	0.26
P_{max}	7.57	2.20	-36.33	17.06	0.19	0.09	-0.02	0.02
α	0.13	0.04	-0.88	0.04	0.00	0.00	0.00	0.00
I_k	83.01	21.72	260.00	202.00	0.91	0.93	0.27	0.23
Respiration	5.78	1.41	-25.52	13.66	0.08	0.07	-0.02	0.02
Chl *a* + *b*	0.20	0.07	-0.19	0.57	0.01	0.00	0.00	0.00
Tissue C	307.51	11.91	-8.00	88.00	0.86	0.78	0.08	0.11
Tissue N	22.40	7.07	-41.00	55.20	0.69	0.63	0.04	0.07
C:N	15.33	3.70	31.87	22.81	-0.32	0.28	-0.02	0.03
$\delta^{15}N$	3.68	0.16	-3.09	1.30	-0.03	0.01	0.00	0.00
$\Delta^{13}C$	-0.54	0.06	0.50	0.62	0.00	0.00	0.00	0.00

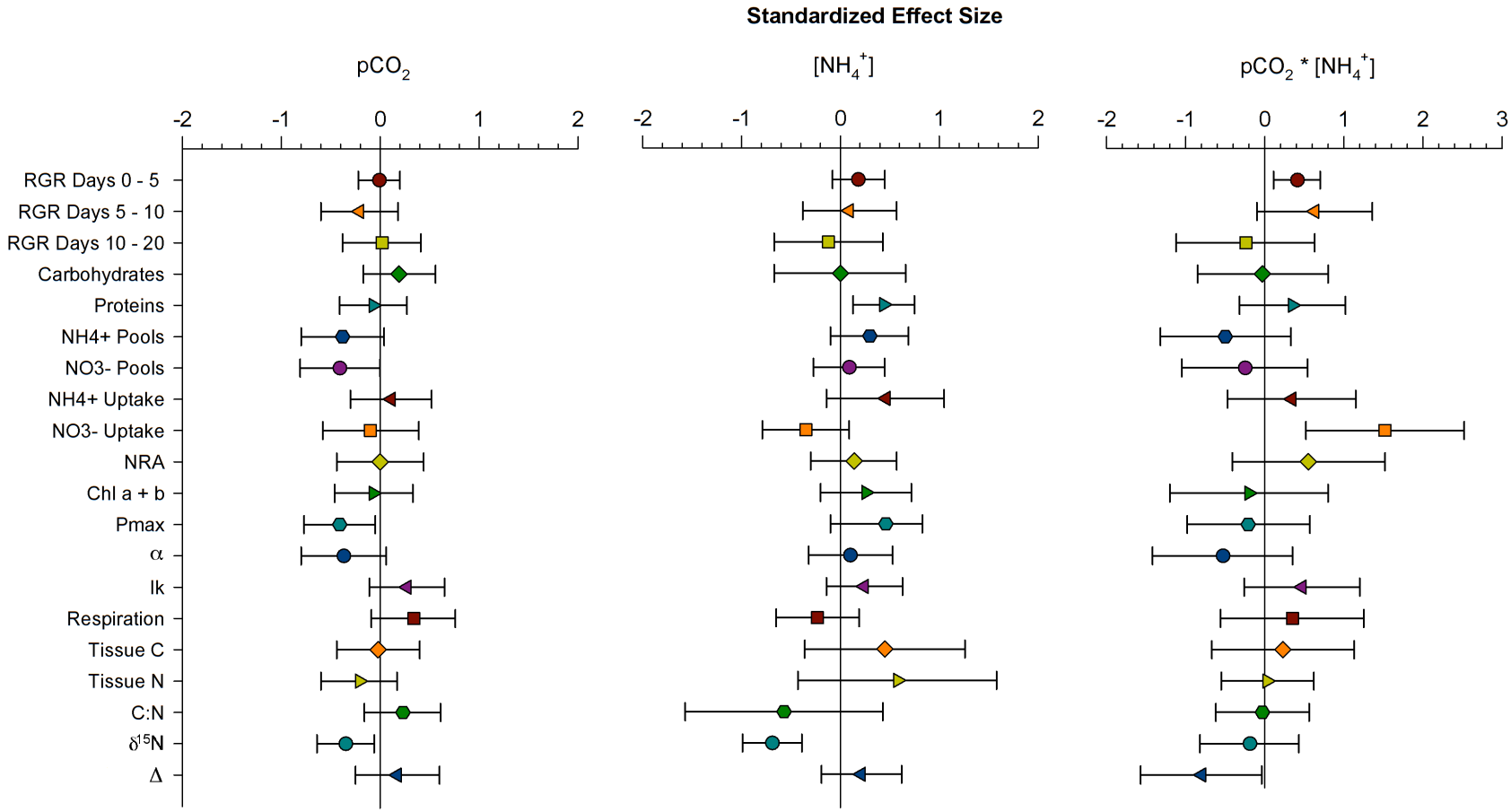

Fig 3.2: Standardized effect sizes for physiological responces of *Ulva lactuca* to ocean acidificiation and eutrophication. The effect sizes were calculated as the weighted average of standardized coefficients from each model in the set (n=23). Error bars are 95% confidence intervals

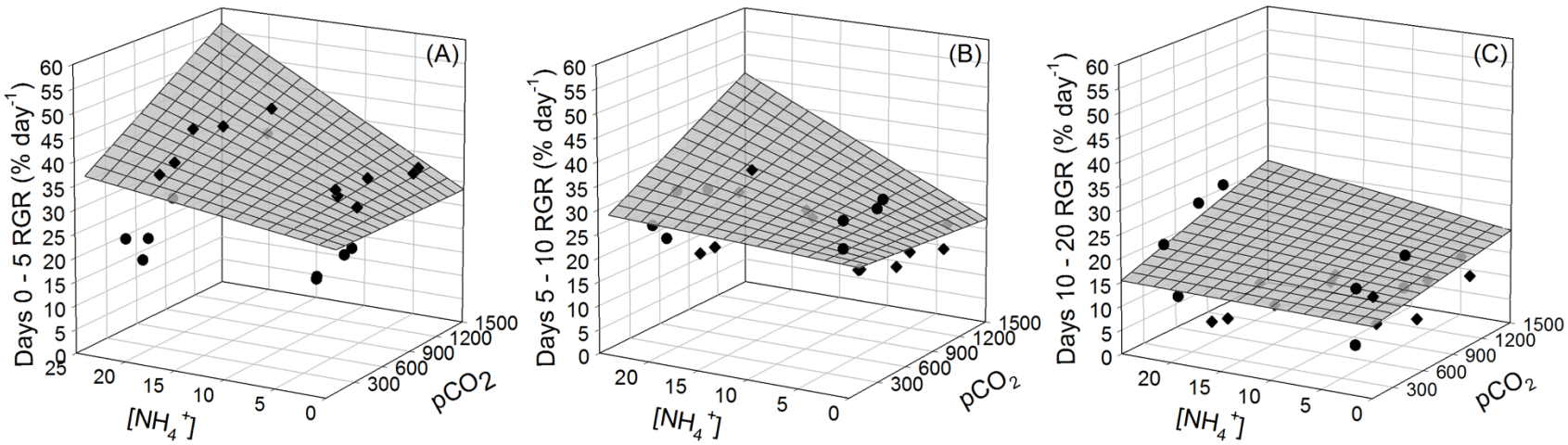

Fig 3.3: Modeled relative growth rates for *Ulva lactuca* over time based on responses to pCO_2 and NH_4^+ treatments in laboratory experiments. (A) Days 0 – 5 (B) Days 5 – 10 (C) Days 10 – 20. (●) Trial 1 (♦) Trial 2. The linear expression $y=\beta_0+(\beta_1*x_1)+(\beta_2*x_2)+(\beta_3*(x_1*x_2))$, where $x_1 = pCO_2$ and $x_2 = [NH_4^+]$, was used to fit model surface with conventional regression coefficients using weighted model-averaging (See Table 3.2).

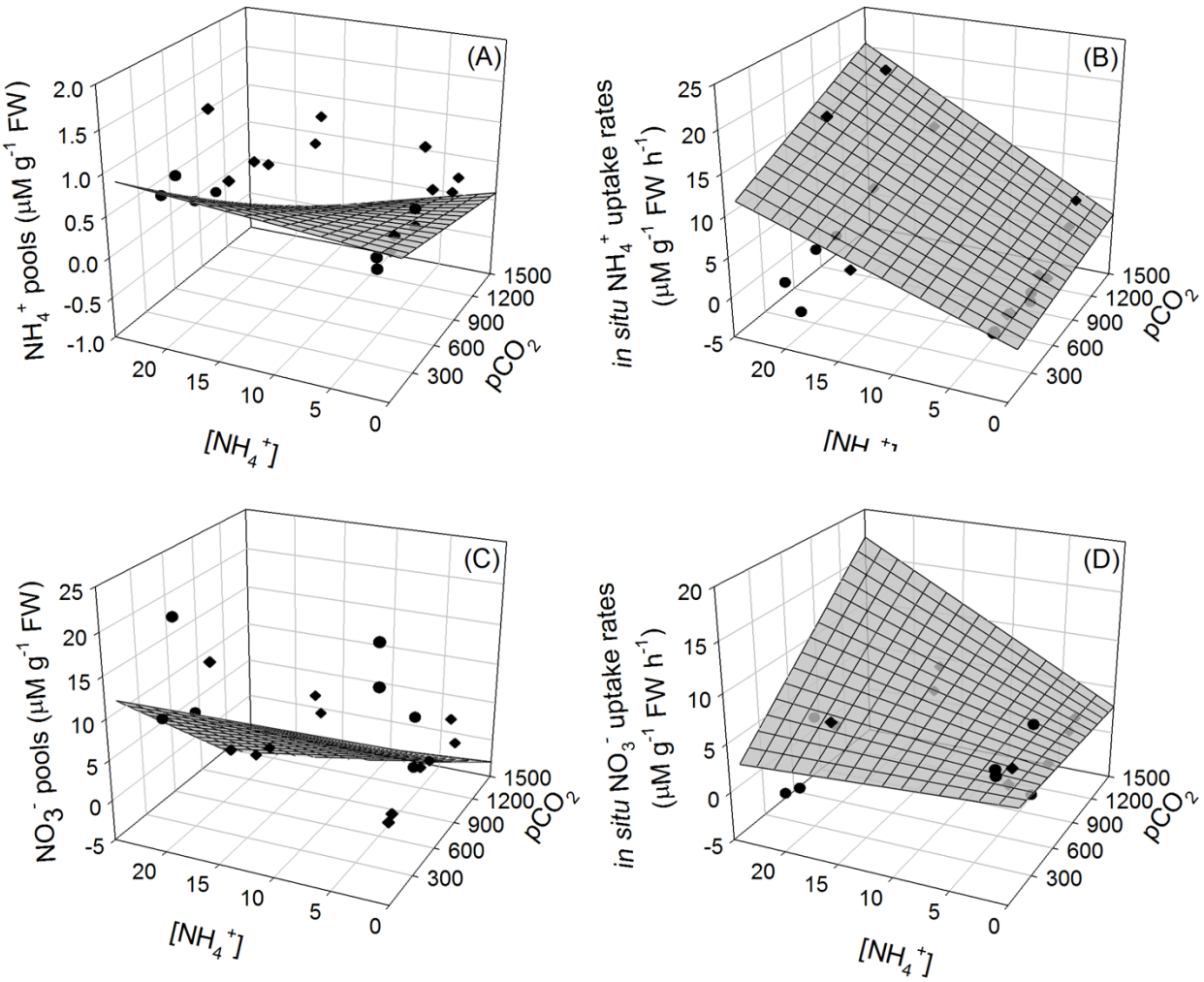

Fig 3.4: Modeled physiological responses for *Ulva lactuca* based on responses to pCO_2 and NH_4^+ treatments in laboratory experiments. (A) NH_4^+ pools (B) *in situ* NH_4^+ uptake rates (C) NO_3^- pools and (D) *in situ* NO_3^- uptake rates. (●) Trial 1 (♦) Trial 2. The linear expression $y=\beta_0+(\beta_1*x_1)+(\beta_2*x_2)+(\beta_3*(x_1*x_2))$, where $x_1 = pCO_2$ and $x_2 = [NH_4^+]$, was used to fit model surface with conventional regression coefficients using weighted model-averaging (See Table 3.2).

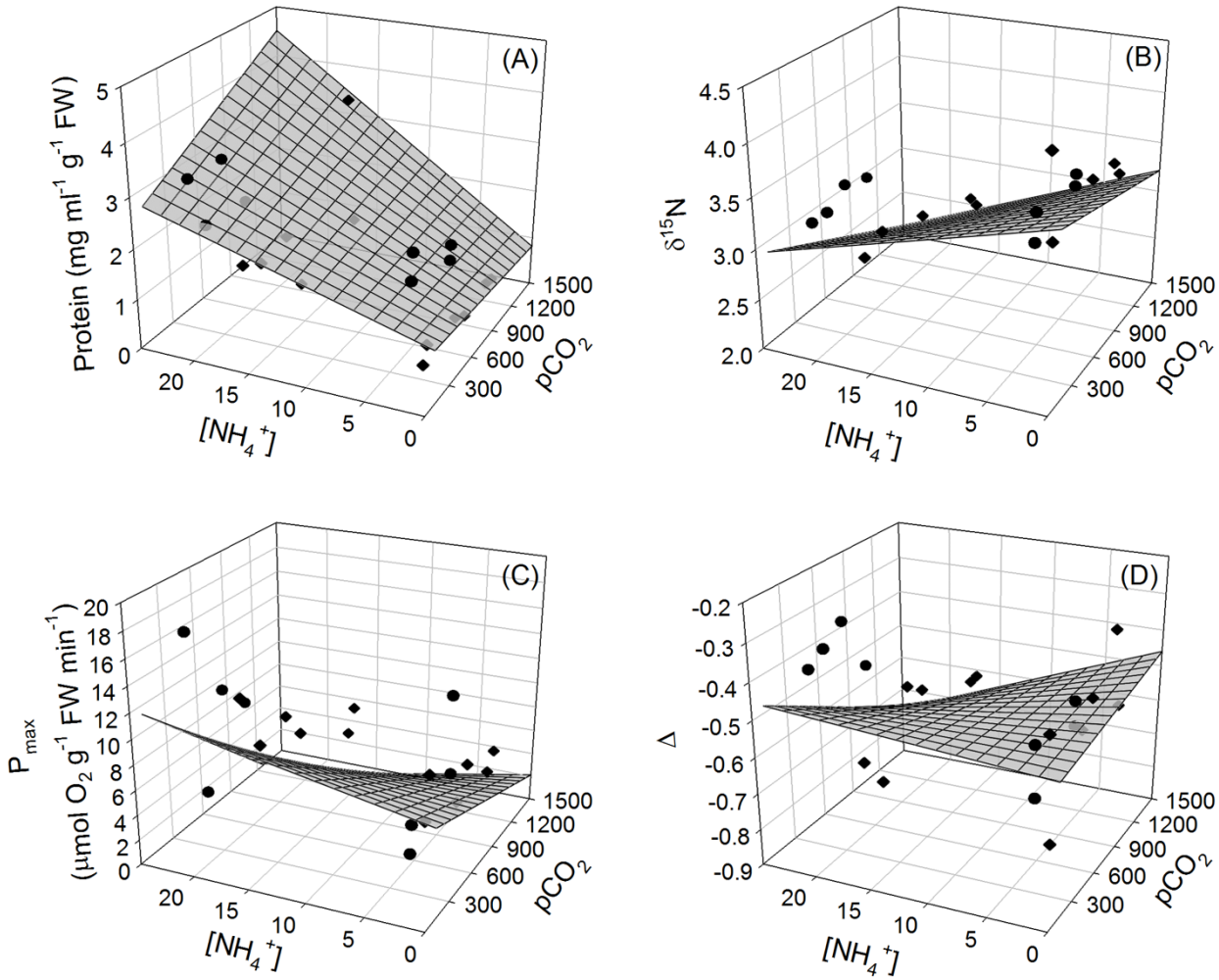

Fig 3.5: Modeled physiological responses for *Ulva lactuca* based on responses to pCO_2 and NH_4^+ treatments in laboratory experiments. (A) Soluble protein concentrations (B) $\delta^{15}N$ (C) Pmax and (D) Δ. (●) Trial 1 (♦) Trial 2. The linear expression $y=\beta_0+(\beta_1*x_1)+(\beta_2*x_2)+(\beta_3*(x_1*x_2))$, where $x_1 = pCO_2$ and $x_2 = [NH_4^+]$, was used to fit model surface with conventional regression coefficients using weighted model-averaging (See Table 3.2).

Literature Cited

Alexandre A, Silva J, Buapet P, Björk M, Santos R (2012) Effects of CO_2 enrichment on photosynthesis, growth, and nitrogen metabolism of the seagrass *Zostera noltii*. Ecol Evol 2:2625–2635. doi: 10.1002/ece3.333

Anderson DM, Glibert P, Burkholder J (2002) Harmful algal blooms and eutrophication: Nutrient sources, compositions, and consequences. Estuaries 25:704–726. doi: 10.1016/j.hal.2008.08.017

Anderson DR (2009) Model based inferences in the life sciences: A Primer on evidence. Springer, New York

Andría JR, Vergara J, Perez-Llorens JL (1999) Biochemical responses and photosynthetic performance of *Gracilaria* sp. (Rhodophyta) from Cadiz, Spain, cultured under different inorganic carbon and nitrogen levels. Eur J Phycol 34:497–504. doi: 10.1080/09541449910001718851

Andría JR, Brun FG, Pérez-Lloréns JL, Vergara JJ (2001) Acclimation responses of *Gracilaria* sp. (Rhodophyta) and *Enteromorpha intestinalis* (Chlorophyta) to changes in the external inorganic carbon concentration. Bot Mar 44:361–370. doi: 10.1515/BOT.2001.046

Axelsson L, Larsson C, Ryberg H (1999) Affinity, capacity and oxygen sensitivity of two different mechanisms for bicarbonate utilization in *Ulva lactuca* L. (Chlorophyta). Plant, Cell Environ 22:969–978. doi: 10.1046/j.1365-3040.1999.00470.x

Baker NR (2008) Chlorophyll fluorescence: A probe of photosynthesis in vivo. Annu Rev Plant Biol 59:89–113. doi: 10.1146/annurev.arplant.59.032607.092759

Barr NG (2007) Aspects of nitrogen metabolism in the green alga *Ulva*; Developing an indicator of seawater nitrogen loading. Univ Auckland, PhD thesis 1994:1–219.

Beardall J, Beer S, Raven JA (1998) Biodiversity of marine plants in an era of climate change: Some predictions based on physiological performance. Bot Mar 41:113–123. doi: 10.1515/botm.1998.41.1-6.113

Beer S, Koch E (1996) Photosynthesis of marine macroalgae and seagrasses in globally changing CO_2 environments. Mar Ecol Prog Ser 141:199–204. doi: 10.3354/meps141199

Bender-Champ D, Diaz-Pulido G, Dove S (2017) Effects of elevated nutrients and CO_2 emission scenarios on three coral reef macroalgae. Harmful Algae 65:40–51. doi: 10.1016/j.hal.2017.04.004

Björk M, Haglund K, Ramaznov Z, Pedersén M (1993) Inducible mechanisms for HCO_3^- utilisation and repression of photorespiration in protoplasts and thalli of three species of *Ulva*. J Phycol 29:166–173. doi: 10.1111/j.0022-3646.1993.00166.x

Bockmon EE, Frieder CA, Navarro MO, White-Kershek LA, Dickson AG (2013) Technical Note: Controlled experimental aquarium system for multi-stressor investigation of carbonate chemistry, oxygen saturation, and temperature. Biogeosciences 10:5967–5975. doi: 10.5194/bg-10-5967-2013

Bowes G (1991) Growth at elevated CO_2: Photosynthetic responses mediated through Rubisco. Plant Cell Environ 795–806. doi: 10.1111/j.1365-3040.1991.tb01443.x

Bradford MM (1976) A rapid and sensitive method for the quantitation of microgram quantities of protein utilizing the principle of protein-dye binding. Anal Biochem 72:248–254. doi: 10.1016/0003-2697(76)90527-3

Bricker SB, Longstaff BJ, Dennison W, Jones A, Boicourt K, Wicks C, Woerner J (2008) Effects of nutrient enrichment in the nation's estuaries: A decade of change. Harmful Algae 8:21–32. doi: 10.1016/j.hal.2008.08.028

Caldeira K (2005) Ocean model predictions of chemistry changes from carbon dioxide emissions to the atmosphere and ocean. J Geophys Res 110:1–12. doi: 10.1029/2004JC002671

Carmona R, Vergara JJ, Pérez-Lloréns JL, Figueroa FL, Niell FX (1996) Photosynthetic acclimation and biochemical responses of *Gelidium sesquipedale* cultured in chemostats under different qualities of light. Mar Biol 127:25–34. doi: 10.1007/BF00993640

Chan AY, Lubarsky K, Judy KN, Fong P (2012) Nutrient addition increases consumption rates of tropical algae with different initial palatabilities. Mar Ecol Prog Ser 465:25–31. doi: 10.3354/meps09946

Chen B, Zou D, Jiang H (2015) Elevated CO_2 exacerbates competition for growth and photosynthesis between *Gracilaria lemaneiformis* and *Ulva lactuca*. Aquaculture 443:49–55. doi: 10.1016/j.aquaculture.2015.03.009

Cornwall CE, Hepburn CD, Pritchard D, Currie KI, McGraw CM, Hunter KA, Hurd CL (2012) Carbon-use strategies in macroalgae: Differential responses to Lowered pH and implications for ocean acidification. J Phycol 48:137–144. doi: 10.1111/j.1529-8817.2011.01085.x

Cornwall CE, Revill AT, Hurd CL (2015) High prevalence of diffusive uptake of CO_2 by macroalgae in a temperate subtidal ecosystem. Photosynth Res 124:181–190. doi: 10.1007/s11120-015-0114-0

Crossett K, Culliton T, Wiley P, Goodspeed T (2005) Population trends along the coastal united states:1980 – 2008. Government Printing Office.

D'Elia CF, DeBoer JA. (1978) Nutritional studies of two red algae. II. Kinetics of ammonium and nitrate uptake. J Phycol 14:266–272. doi: 10.1111/j.1529-8817.1978.tb00297.x

Dailer ML, Smith JE, Smith CM (2012) Responses of bloom forming and non-bloom forming macroalgae to nutrient enrichment in Hawai'i, USA. Harmful Algae 17:111–125. doi: 10.1016/j.hal.2012.03.008

Delille B, Borges AV (2009) Influence of giant kelp beds (*Macrocystis pyrifera*) on diel cycles of pCO_2 and DIC in the Sub-Antarctic coastal area. Estuar Coast Shelf Sci 81:114–122. doi: 10.1016/j.ecss.2008.10.004

Dickson AG, Sabine CL, Christian JR (2007). Guide to Best Practices for Ocean CO_2 Measurements.

Doney SC, Fabry VJ, Feely RA, Kleypas JA (2009) Ocean acidification: the other CO_2 problem. Ann Rev Mar Sci 1:169–192. doi: 10.1146/annurev.marine.010908.163834

Duarte CM, Hendriks IE, Moore TS, Olsen YS, Steckbauer A, Ramojo L, Carstensen J, Trotter JA, McCulloch M (2013) Is ocean acidification an open-ocean syndrome? Understanding anthropogenic impacts on seawater pH. Estuaries and Coasts 36:221–236. doi: 10.1007/s12237-013-9594-3

Fabry VJ, Seibel BA, Feely RA, Orr JC (2008) Impacts of ocean acidification on marine fauna and ecosystem processes. ICES J Mar Sci 65:414. doi: 10.1093/icesjms/fsn048

Falkenberg LJ, Connell SD, Russell BD (2014) Herbivory mediates the expansion of an algal habitat under nutrient and CO_2 enrichment. Mar Ecol Prog Ser 497:87–92. doi: 10.3354/meps10557

Fan X, Xu D, Wang Y, Zhang X, Cao S, Mou S, Ye N (2014) The effect of nutrient concentrations, nutrient ratios and temperature on photosynthesis and nutrient uptake by *Ulva prolifera*: Implications for the explosion in green tides. J Appl Phycol 26:537–544. doi: 10.1007/s10811-013-0054-z

Fong P, Boyer KE, Zedler JB (1998) Developing an indicator of nutrient enrichment in coastal estuaries and lagoons using tissue nitrogen content of the opportunistic alga, *Enteromorpha intestinalis* (L. Link). J Exp Mar Bio Ecol 231:63–79. doi: 10.1016/S0022-0981(98)00085-9

Fong P, Boyer KE, Kamer K, Boyle KA. (2003) Influence of initial tissue nutrient status of tropical marine algae on response to nitrogen and phosphorus additions. Mar Ecol Prog Ser 262:111–123. doi: 10.3354/meps262111

Fong P, Fong JJ, Fong CR (2004) Growth, nutrient storage, and release of dissolved organic nitrogen by *Enteromorpha intestinalis* in response to pulses of nitrogen and phosphorus. Aquat Bot 78:83–95. doi: 10.1016/j.aquabot.2003.09.006

Frankignoulle M, Bouquegneau JM (1990) Daily and yearly variations of total inorganic carbon in a productive coastal area. Estuar Coast Shelf Sci 30:79–89. doi: 10.1016/0272-7714(90)90078-6

Fujita RM (1985) The role of nitrogen status in regulating ammonium transient uptake and nitrogen storage by macroalgae. J Exp Mar Bio Ecol 92:283–301. doi: 10.1016/0022-0981(85)90100-5

Gao K, Aruga Y, Asada K, Kiyohara M (1993) Influence of enhanced CO_2 on growth and photosynthesis of the red algae *Gracilaria* sp. and *G. chilensis*. J Appl Phycol 5:563–571.

Gao S, Chen X, Yi Q, Wang G, Pan G, Lin A, Peng G (2010) A strategy for the proliferation of *Ulva prolifera*, main causative species of green tides, with formation of sporangia by fragmentation. PLoS One 5:1–7. doi: 10.1371/journal.pone.0008571

Gao G, Liu Y, Li X, Feng Z, Xu J (2016) An ocean acidification acclimatised green tide alga is robust to changes of seawater carbon chemistry but vulnerable to light stress. 1–16. doi: 10.1371/journal.pone.0169040

Garcia-Sanchez MJ, Fernandez JA, Niell X (1994) Effect of inorganic carbon supply on the photosynthetic physiology of *Gracilaria tenuistipitata*. Planta 194:55–61. doi: 10.1007/BF00201034

Ghedini G, Russell BD, Connell SD (2015) Trophic compensation reinforces resistance: Herbivory absorbs the increasing effects of multiple disturbances. Ecol Lett 18:182–187. doi: 10.1111/ele.12405

Giordano M, Beardall J, Raven JA (2005) CO_2 concentrating mechanisms in algae: mechanisms, environmental modulation, and evolution. Annu Rev Plant Biol 56:99–131. doi: 10.1146/annurev.arplant.56.032604.144052

Gordillo FJL, Niell FX, Figueroa FL (2001) Non-photosynthetic enhancement of growth by high CO_2 level in the nitrophilic seaweed *Ulva rigida* C. Agardh (Chlorophyta). Plantad 213:64–70. doi: 10.1007/s004250000468

Gordillo FJL, Figueroa FL, Niell FX (2003) Photon- and carbon-use efficiency in *Ulva rigida* at different CO_2 and N levels. Planta 218:315–322. doi: 10.1007/s00425-003-1087-3

Guiry MD, Guiry GM (2016) World-wide electronic publication, National University of Ireland, Galway. http://www.algaebase.org.

Henley WJ, Levavasseur G, Franklin LA, Osmond B, Ramus L (1991) Photoacclimation and Photoinhibition in Ulva rotundata as influenced by nitrogen availability. Planta 184:235–243. doi: 10.1007/BF00197952

Hepburn CD, Pritchard DW, Cornwall CE, McLeod RJ, Beardall J, Raven JA, Hurd CL (2011) Diversity of carbon use strategies in a kelp forest community: Implications for a high CO_2 ocean. Glob Chang Biol 17:2488–2497. doi: 10.1111/j.1365-2486.2011.02411.x

Holmes RM, Aminot A, Kérouel R, Hooker BA, Peterson B (1999) A simple and precise method for measuring ammonium in marine and freshwater ecosystems. Can J Fish Aquat Sci 56:1801–1808.

Hurd CL, Harrison PJ, Druehl LD (1996) Effect of seawater velocity on inorganic nitrogen uptake by morphologically distinct forms of *Macrocystis integrifolia* from wave-sheltered and exposed sites. Mar Biol 126:205–214. doi: 10.1007/BF00347445

Hurd CL (2000) Water motion, marine macroalgal physiology, and production. J Phycol 36:453–472. doi: 10.1046/j.1529-8817.2000.99139.x

Hurd CL, Hepburn CD, Currie KI, Raven JA, Hunter KA (2009) Testing the effects of ocean acidification on algal metabolism: Considerations for experimental designs. J Phycol 45:1236–1251. doi: 10.1111/j.1529-8817.2009.00768.x

IPCC (2013) Climate Change 2013: The physical science basis. Contribution of working group I to the fifth assessment report of the intergovernmental panel on climate change. Cambridge University Press

IPCC (2015) Climate Change 2014: Mitigation of Climate Change Vol 3. Cambridge University Press

Israel A, Hophy M (2002) Growth, photosynthetic properties and Rubisco activities and amounts of marine macroalgae grown under current and elevated seawater CO_2 concentrations. Glob Chang Biol 8:831–840. doi: 10.1046/j.1365-2486.2002.00518.x

Johnson MD, Price NN, Smith JE (2014) Contrasting effects of ocean acidification on tropical fleshy and calcareous algae. PeerJ 2:e411. doi: 10.7717/peerj.411

Kennison RL, Kamer K, Fong P (2011) Rapid nitrate uptake rates and large short-term storage capacities may explain why opportunistic green macroalgae dominate shallow eutrophic estuaries. J Phycol 47:483–494. doi: 10.1111/j.1529-8817.2011.00994.x

Kennison RL, Fong P (2014) Extreme eutrophication in shallow estuaries and lagoons of California is driven by a unique combination of local watershed modifications that trump variability associated with wet and dry seasons. Estuaries and Coasts 37:164–179. doi: 10.1007/s12237-013-9687-z

Koch M, Bowes G, Ross C, Zhang XH (2013) Climate change and ocean acidification effects on seagrasses and marine macroalgae. Glob Chang Biol 19:103–132. doi: 10.1111/j.1365-2486.2012.02791.x

Kochert, G (1978) Carbohydrate determination by the phenol sulfuric acid method. In: Hellbust JA, Craigie JS (eds) Handbook of phycological methods: Physiological and biochemical methods. Cambridge University Press, Cambridge, pp 95-97.

Kroeker KJ, Kordas RL, Crim RN, Hendricks IE, Ramajo L, Singh GS, Duarte CM, Gattuso JP (2013) Impacts of ocean acidification on marine organisms: Quantifying sensitivities and interaction with warming. Glob Chang Biol 19:1884–1896. doi: 10.1111/gcb.12179

Kübler JE, Raven JA (1995) The interaction between inorganic carbon acquisition and light supply in *Palmaria palmata* (Rhodophyta). J Phycol 31:369–375. doi: 10.1111/j.0022-3646.1995.00369.x

Kübler JE, Johnston AM, Raven JA (1999) The effects of reduced and elevated CO_2 and O_2 on the seaweed *Lomentaria articulata*. Plant Cell Environ 22:1303–1310. doi: 10.1046/j.1365-3040.1999.00492.x

Kübler JE, Dudgeon SR (2015) Predicting effects of ocean acidification and warming on algae lacking carbon concentrating mechanisms. PLoS One 10:1–19. doi: 10.1371/journal.pone.0132806

Lapointe BE, Tenore KR (1981) Experimental outdoor studies with *Ulva fasciata* Delile. I. Interaction of light and nitrogen on nutrient uptake, growth, and biochemical composition. J Exp Mar Bio Ecol 53:135–152. doi: 10.1016/0022-0981(81)90015-0

Lavigne H, Epitalon, JM, Gattuso JP, 2011. Seacarb: seawater carbonate chemistry with R. R package version 3.0. http://CRAN.R-project.org/package=seacarb

Li S, Yu K, Huo Y, Zhang J, Wu H, Cai C, Liu Y, Shi D, He P (2016) Effects of nitrogen and phosphorus enrichment on growth and photosynthetic assimilation of carbon in a green tide-forming species (Ulva prolifera) in the Yellow Sea. Hydrobiologia 776:161–171. doi: 10.1007/s10750-016-2749-z

Li ZP, Tao MX, Li LW, Wang, ZD, Du L, Zhang MF (2007) Determination of isotope composition of dissolved organic carbon by gas chromatography- conventional isotope-ratio mass spectrometry. Chin. J. Anal. Chem. 35: 1455-1458. doi: 10.1016/S1872-2040(07)60089-9

Littler MM, Littler DS (1980) The evolution of thallus form and survival strategies in benthic marine macroalgae: Field and laboratory tests of a functional form model. Am Nat 116:25–44. doi: 10.1086/283610

Liu D, Keesing JK, Xing Q, Shi P (2009) World's largest macroalgal bloom caused by expansion of seaweed aquaculture in China. Mar Pollut Bull 58:888–895. doi: 10.1016/j.marpolbul.2009.01.013

Liu C, Zou D (2015) Effects of elevated CO_2 on the photosynthesis and nitrate reductase activity of *Pyropia haitanensis* (Bangiales, Rhodophyta) grown at different nutrient levels. Chinese J Oceanol Limnol 33:419–429. doi: 10.1007/s00343-015-4057-2

Lüthi D, Le Floch M, Bereiter B, et al (2008) High-resolution carbon dioxide concentration record 650,000-800,000 years before present. Nature 453:379–382. doi: 10.1038/nature06949

Maberly SC, Raven JA, Johnston AM (1992) Discrimination between C^{12} and C^{13} by marine plants. Oecologia 91:481–492. doi: 10.1007/BF00650320

Mazerolle MJ. (2013) Model selection and multimodel inference based on (Q)AIC(c). R Package, Version 1.35 2013.

McElhany P, Shallin Busch D (2013) Appropriate pCO_2 treatments in ocean acidification experiments. Mar Biol 160:1807–1812. doi: 10.1007/s00227-012-2052-0

McGlathery KJ, Pedersen MF, Borum J (1996) Changes in intracellular nitrogen pools and feedback controls on nitrogen uptake in *Chaetomorpha linum (*Chlorophyta). J Phycol 32:393–401. doi: 10.1111/j.0022-3646.1996.00393.x

McGraw CM, Cornwall CE, Reid MR, Currie KI, Hepburn CD, Boyd, P, Hurd CL, Hunter KA (2010) An automated pH-controlled culture system for laboratory-based ocean acidification experiments. Limnol Oceanogr Methods 8:686–694. doi: 10.4319/lom.2010.8.686

Middelboe AL, Hansen PJ (2007) High pH in shallow-water macroalgal habitats. Mar Ecol Prog Ser 338:107–117. doi: 10.3354/meps338107

Miflin BJ, Lea PJ (1976) The pathway of nitrogen assimilation in plants. Phytochemistry 15:873–885. doi: 10.1016/S0031-9422(00)84362-9

Morand P, Briand X (1996) Excessive growth of macroalgae: A symptom of environmental disturbance. Bot Mar 39:491–516. doi: 10.1515/botm.1996.39.1-6.491

Naldi M, Viaroli P (2002) Nitrate uptake and storage in the seaweed *Ulva rigida* C. Agardh in relation to nitrate availability and thallus nitrate content in a eutrophic coastal lagoon (Sacca di Goro, Po River Delta, Italy). J Exp Mar Bio Ecol 269:65–83. doi: 10.1016/S0022-0981(01)00387-2

Olischläger M, Bartsch I, Gutow L, Wiencke C (2013) Effects of ocean acidification on growth and physiology of *Ulva lactuca* (Chlorophyta) in a rockpool-scenario. Phycol Res 61:180–190. doi: 10.1111/pre.12006

Paerl HW (1997) Coastal eutrophication and harmful algal blooms: Importance of atmospheric deposition and groundwater as new nitrogen and other nutrient sources. Limnol Oceanogr 42:1154–1165. doi: 10.4319/lo.1997.42.5_part_2.1154

Paerl HW, Piehler MF (2008) Nitrogen and marine eutrophication. In: Carpenter EJ, Capon DG (eds) Nitrogen in the marine environment. Academic Press, Orlando, pp 593–601.

Pedersen MF (1994) Transient ammonium uptake in the macroalgae *Ulva lactuca* (Chlorophyta): Nature, regulation, and the consequences for choice of measuring technique. J Phycol 30:980–986. doi: 10.1111/j.0022-3646.1994.00980.x

Pedersen MF, Borum J (1996) Nutrient control of algal growth in estuarine waters. Nutrient limitation and the importance of nitrogen requirements and nitrogen storage among phytoplankton and species of macroalgae. Mar Ecol Prog Ser 142:261-272. doi: 10.3354/meps142261

Pedersen, MF, Borum J (1997) Nutrient control of estuarine macroalgae: Growth strategy and the balance between nitrogen requirements and uptake. Mar Ecol Prog Ser 161:155–163. doi: 10.3354/meps161155

Perrot T, Rossi N, Ménesguen A, Dumas F (2014) Modelling green macroalgal blooms on the coasts of Brittany, France to enhance water quality management. J Mar Syst 132:38–53. doi: 10.1016/j.jmarsys.2013.12.010

Provasoli L (1968) Media and prospects for the cultivation of marine algae. In: Watanabe A, Hattori A (eds) Cultures and collections of algae (Proc. U.S.- Japan Conf., Hakone), Jpn Soc Plant Physiol pp 63-75

Rautenberger R, Fernández PA., Strittmatter M, Heesch S, Cornwall CE, Hurd CL, Roleda MY (2015) Saturating light and not increased carbon dioxide under ocean acidification drives photosynthesis and growth in *Ulva rigida* (Chlorophyta). Ecol Evol 5:874–888. doi: 10.1002/ece3.1382

Raven JA (1997) Putting the C in phycology. Eur J Phycol 32:319–333. doi: 10.1017/s0967026297001388

Raven JA, Johnston AM, Kübler JE, et al (2002) Mechanistic interpretation of carbon isotope discrimination by marine macroalgae and seagrasses. Funct Plant Biol 29:335–378. doi: 10.1071/PP01201

Raven JA, Caldeira K, Elderfield H, et al (2005) Ocean acidification due to increasing atmospheric carbon dioxide. The Royal Society, London.

Raven JA, Giordano M, Beardall J, Maberly SC (2011) Algal and aquatic plant carbon concentrating mechanisms in relation to environmental change. Photosynth Res 109:281–296. doi: 10.1007/s11120-011-9632-6

Raven JA, Giordano M, Beardall J, Maberly SC (2012) Algal evolution in relation to atmospheric CO_2: carboxylases, carbon-concentrating mechanisms and carbon oxidation cycles. doi: 10.1098/rstb.2011.0212

Ritchie RJ (2008) Universal chlorophyll equations for estimating chlorophylls *a*, *b*, *c*, and *d* and total chlorophylls in natural assemblages of photosynthetic organisms using acetone, methanol, or ethanol solvents. Photosynthetica 46:115–126. doi: 10.1007/s11099-008-0019-7

Sharp, JH (1983) The distributions of inorganic nitrogen, and dissolved and particulate organic nitrogen in the sea. In: Carpenter EJ, Capone DG (eds) Nitrogen in the marine environment. Academic Press, New York, pp 1-35

Smetacek V, Zingone A (2013) Green and golden seaweed tides on the rise. Nature 504:84–8. doi: 10.1038/nature12860

Smith SV, Swaney DP, Talaue-McManus L, et al (2003) Humans, Hydrology, and the Distribution of Inorganic Nutrient Loading to the Ocean. Bioscience 53:235. doi: 10.1641/0006-3568(2003)053[0235:HHATDO]2.0.CO;2

Stengel DB, Conde-Álvarez R, Connan S, et al (2014) Short-term effects of CO_2, nutrients and temperature on three marine macroalgae under solar radiation. Aquat Biol 22:159–176. doi: 10.3354/ab00576

Stepien CC (2015) Impacts of geography, taxonomy and functional group on inorganic carbon use patterns in marine macrophytes. J Ecol 103:1372–1383. doi: 10.1111/1365-2745.12451

Stitt M, Krapp A (1999) The interaction between elevated carbon dioxide and nitrogen nutrition: the physiological and molecular background. Plant Cell Environ 22:553–621. doi: 10.1046/j.1365-3040.1999.00386.x

Suárez-Álvarez S, Gomez-Pinchetti JL, Garcia-Reina G (2012) Effects of increased CO_2 levels on growth, photosynthesis, ammonium uptake and cell composition in the macroalga *Hypnea spinella* (Gigartinales, Rhodophyta). J Appl Phycol 24:815–823. doi: 10.1007/s10811-011-9700-5

Syrett PJ (1981) Nitrogen Metabolism of Microalgae. Can J Fish Aquat Sci 210:182–210.

Taylor BW, Keep CF, Hall RO, Koch BJ, Tronstad LM, Flecker AS, Ulseth AJ (2007) Improving the fluorometric ammonium method: Matrix effects, background fluorescence, and standard additions. J North Am Benthol Soc 26:167–177. doi: 10.1899/0887-3593(2007)26[167:ITFAMM]2.0.CO;2

Teichberg M, Heffner LR, Fox S, Valiela I (2007) Nitrate reductase and glutamine synthetase activity, internal N pools, and growth of *Ulva lactuca*: Responses to long and short-term N supply. Mar Biol 151:1249–1259. doi: 10.1007/s00227-006-0561-4

Teichberg M, Fox SE, Aguila C, et al (2008) Macroalgal responses to experimental nutrient enrichment in shallow coastal waters: Growth, internal nutrient pools, and isotopic signatures. Mar Ecol Prog Ser 368:117–126. doi: 10.3354/meps07564

Teichberg M, Fox SE, Olsen YS, et al (2010) Eutrophication and macroalgal blooms in temperate and tropical coastal waters: Nutrient enrichment experiments with *Ulva* spp. Glob Chang Biol 16:2624–2637. doi: 10.1111/j.1365-2486.2009.02108.x

Thompson SM, Valiela I (1999) Effect of nitrogen loading on enzyme activity of macroalgae in estuaries in waquoit bay. Bot Mar. doi: 10.1515/BOT.1999.059

Todgham AE, Stillman JH (2013) Physiological responses to shifts in multiple environmental stressors: Relevance in a changing world. Integr Comp Biol 53:539–544. doi: 10.1093/icb/ict086

Turpin DH (1991) Effects of Inorganic N availability on algal photosynthesis and carbon metabolism. J. Phycol. 27:14–20.

Valiela I, Mcclelland J, Hauxwell J, Behr PJ, Hersh D, Foreman K (1997) Macroalgal blooms in shallow estuaries: Controls and ecophysiological and ecosystem consequences. Limnol Oceanogr 42:1105–1118. doi: 10.4319/lo.1997.42.5_part_2.1105

Van Alstyne KL, Nelson TA, Ridgway RL (2015) Environmental chemistry and chemical ecology of "green tide" seaweed blooms. Integr Comp Biol 55:518–532. doi: 10.1093/icb/icv035

Vanlerberghe GC, Schuller KA, Smith RG, Feil R, Plaxton WC, Turpin DH (1990) Relationship between NH_4^+ assimilation rate and *in vivo* phosphoenolpyruvate carboxylase activity : Regulation of anaplerotic carbon flow in the green alga *Selenastrum minutum*. Plant Physiol 94:284–90. doi: 10.1104/pp.94.1.284

Vitousek PM, Mooney HA, Lubchenco J, Melillo JM (1997) Human Domination of Earth's Ecosystems. Science 277:494–499. doi: 10.1126/science.277.5325.494

Walsby AE (1997) Numerical integration of phytoplankton photosynthesis through time and depth in a water column. New Phytol 136:189–209. doi: 10.1046/j.1469-8137.1997.00736.x

Wootton JT, Pfister CA, Forester JD (2008) Dynamic patterns and ecological impacts of declining ocean pH in a high-resolution multi-year dataset. Proc Natl Acad Sci USA 105:18848–53. doi: 10.1073/pnas.0810079105

Xu J, Gao K (2012) Future CO_2-induced ocean acidification mediates the physiological performance of a green tide alga. Plant Physiol 160:1762–1769. doi: 10.1104/pp.112.206961

Ye NH, Zhang XW, Mao YZ, Liang CW, Xu D, Zou J, Zhuang Zm, Wang QY (2011) "Green tides" are overwhelming the coastline of our blue planet: Taking the world's largest example. Ecol Res 26:477–485. doi: 10.1007/s11284-011-0821-8

Young CS, Gobler CJ (2016) Ocean acidification accelerates the growth of two bloom-forming macroalgae. PLoS One 11:1–21. doi: 10.1371/journal.pone.0155152

Zou D (2005) Effects of elevated atmospheric CO_2 on growth, photosynthesis and nitrogen metabolism in the economic brown seaweed, *Hizikia fusiforme* (Sargassaceae, Phaeophyta). Aquaculture 250:726–735. doi: 10.1016/j.aquaculture.2005.05.014

Zou D, Gao K (2009) Effects of elevated CO_2 on the red seaweed *Gracilaria lemaneiformis* (Gigartinales , Rhodophyta) grown at different irradiance levels. Phycologia 48:510–517. doi: 10.2216/08-99.1